ISSN 0016-7029, Geochemistry International, 2015, Vol. 53, No. 10, pp. 849–868. © Pleiades Publishing, Ltd., 2015.
Original Russian Text © A.A. Kadik, V.V. Koltashev, E.B. Kryukova, V.G. Plotnichenko, T.I. Tsekhonya, N.N. Kononkova, 2015, published in Geokhimiya, 2015, No. 10, pp. 867–887.

Solubility of Nitrogen, Carbon, and Hydrogen in $FeO–Na_2O–Al_2O_3–SiO_2$ Melt and Liquid Iron Alloy: Influence of Oxygen Fugacity

A. A. Kadik[a], V. V. Koltashev[b], E. B. Kryukova[a, b], V. G. Plotnichenko[b, c], T. I. Tsekhonya[a], and N. N. Kononkova[a]

[a] *Vernadsky Institute of Geochemistry and Analytical Chemistry, Russian Academy of Sciences, ul. Kosygina 19, Moscow, 119991 Russia*
e-mail: kadik@geokhi.ru

[b] *Research Center of Fiber Optics, Russian Academy of Sciences, ul. Vavilova 38, Moscow, 119333 Russia*

[c] *Moscow Institute of Physics and Technology, Institutskii per. 19, Dolgoprudnyi, Moscow oblast, 141700 Russia*

Received November 19, 2014; accepted February 18, 2015

Abstract—Reactions of nitrogen, carbon, and hydrogen with $FeO–Na_2O–Al_2O_3–SiO_2$ melts, liquid iron alloys, and graphite were investigated at 4 GPa, 1550°C, and fO_2 values 1.5–3.0 orders of magnitude below $fO_2(IW)$. A number of features important for the understanding of the formation conditions of volatile nitrogen compounds during melting of the Earth's early reduced mantle were revealed. The nitrogen content of melt increases with decreasing fO_2 from 0.96 wt % at $\Delta\log fO_2(IW) = -1.4$ to 4.1 wt % at $\Delta\log fO_2(IW) = -3.0$, whereas the hydrogen content of melt is weakly dependent on fO_2 and lies within 0.40–0.47 wt %. The carbon content is approximately 0.3–0.5 wt %. The IR and Raman spectroscopy of the glasses indicated that the dissolution of nitrogen, carbon, and hydrogen in silicate liquids is accompanied by the formation of NH_3, N_2, and CH_4 molecules, as well as NH_2^-, NH_2^+, NH_4^+, and CH_3^- complexes. Hydrogen is dissolved in melts as OH^-, H_2O, and H_2. The experiments also demonstrated the presence of species with C=O double bonds in the melts. It was found that the solubility of nitrogen in $FeO–Na_2O–Al_2O_3–SiO_2$ melts increases in the presence of carbon owing to the formation of species with C–N bonds in the silicate liquid. One of the most remarkable features of nitrogen, carbon, and hydrogen interaction with $FeO–Na_2O–Al_2O_3–SiO_2$ melts is a significant change in the proportions of N–C–H–O species at fO_2 2–3 orders of magnitude below $fO_2(IW)$. Under these conditions, a sharp decrease in the contents of NH_4^+, NH_2^+ (O–NH_2), OH, H_2O, and CH_4 is accompanied by enrichment in NH_2^- (≡Si–NH_2) and NH_3. As a result, NH_3 becomes the dominant nitrogen species in the melt. The investigation revealed high nitrogen solubility in iron alloys at $fO_2 < fO_2(IW)$. The nitrogen content increases from 2.47 wt % at $\Delta\log fO_2(IW) = -1.4$ to 3.63 wt % at $\Delta\log fO_2(IW) = -3.0$. The carbon content of N–C–Fe alloys ranges from 2.3 to 3.8 wt % and decreases with decreasing fO_2. The siderophile behavior of nitrogen at $fO_2 < fO_2(IW)$ suggests that part of nitrogen could be dissolved in iron alloys during large-scale melting of the early reduced mantle with subsequent nitrogen burial in the Earth's metallic core. It was suggested that the self-oxidation of magmas in the Earth's early mantle with the release of reduced N–C–H–O volatiles could be one of the reasons of extensive nitrogen degassing.

Keywords: nitrogen, carbon, hydrogen, oxygen fugacity, Earth's early mantle, magma ocean, iron alloy, degassing

DOI: 10.1134/S001670291510002X

PROBLEM FORMULATION

The behavior of nitrogen during the chemical differentiation of terrestrial materials is still a topic of debate (e.g., Javoy, 1997; Cartigny et al., 2001; Marty and Dauphas, 2003; Marty, 2012). Nitrogen is the main component of the Earth's present-day atmosphere, but the early atmosphere could be dramatically different (Catling amd Claire, 2005; Shaw, 2008; Zahnle et al., 2010). Its gas components were probably NH_3, CH_4, H_2, and H_2O. It was suggested that the reduced atmosphere could be a source of prebiotic molecules, whose formation had led to the origin of life on Earth (e.g., Galimov, 2004).

The evaluation of the geochemical history of nitrogen and formation of its possible mantle reservoirs is strongly hindered by the poor knowledge of the influence of temperature, pressure, and redox conditions on the distribution of nitrogen among the mantle, core, products of planetary melting, and a deep fluid phase.

Important characteristics of nitrogen behavior can be gained from the experimental investigations of nitrogen dissolution in minerals, silicate and metallic melts, and fluids under mantle pressures. In particular, it was shown that nitrogen could be incorporated under mantle conditions in some silicates and spinels as the osbornite component or in aluminum-bearing silicates (Watenphul et al., 2009). The stability of iron nitrides at high temperatures and pressures (Adler and Williams, 2005; Hasegawa and Yagi, 2005) makes them viable candidates for the formation of nitrogen reservoirs in the mantle and core. The experiments of Watenphul et al. (2010) and Li et al. (2013) suggested that nitrogen could be dissolved in the products of magma ocean crystallization and be retained, thus, in the minerals of the Earth's early mantle. Li and Keppler (2014) concluded that NH_3 is the dominant nitrogen compound in the deep parts of the reduced mantle.

One of the endogenic sources of nitrogen, carbon, and hydrogen in the early atmosphere is the gas exchange between the zones of extensive mantle melting (magma ocean) and the surface of the early Earth. The magma ocean was connected with the forming planetary core through the gravitational migration of metallic iron in the molten silicate mantle (Li and Agee, 1996; Righter and Drake, 2000; Wood et al., 2006; Frost et al., 2008). The segregation of the core had to be accompanied by the formation of volatile compounds in the zones of large-scale melting of the early Earth; their composition was controlled by the interaction of C, N, H, and O with silicate and metallic melts. Therefore, the gas regime of the early Earth had to be related to the character of dissolution of volatile components in silicate and metallic melts at fO_2 values 4–8 orders of magnitude lower than those characteristic of present-day mantle magmas. The speciation of N, C, H, and O in silicate and metallic phases can be experimentally determined at fO_2 values prevailing during the formation and evolution of the magma ocean.

The influence of pressure, oxygen fugacity (fO_2), and hydrogen fugacity (fH_2) on the solubility of N–H–O volatile compounds in silicate melts was studied by Fogel (1994), Libourel et al. (2003), Miyazaki et al. (2004), Roskosz et al. (2006), Mysen et al. (2008, 2014); Mysen and Fogel (2010), Mysen (2013), and Kadik et al. (2011, 2013). Under reducing conditions, the chemical interaction of nitrogen with hydrogen and silicate liquid components produces N–H species (NH_3, NH_2^-, and NH_2^+), among which the NH_3 molecule can be dominant at fO_2 below the Fe–FeO (IW) buffer equilibrium. Hence, it can be suggested that reduced magmas were the source of NH_3 for the reduced atmosphere (e.g., Roskosz et al., 2006; Kadik et al., 2011, 2013; Mysen, 2012; Li and Keppler, 2014). The experiments of Kadik et al. (2011, 2013) and Roskosz et al. (2013) established for the first time a significant decrease in nitrogen partition coefficient between metal and silicate liquid at high pressures. This effect could be the reason for the depletion of nitrogen relative to other volatiles in the bulk Earth composition, which was detected by Marty (2012). Experimental investigations of the solubility of C–O–H compounds in silicate melts at $fO_2 < fO_2$ (*IW*) established the formation of C–H species in them (CH_4, CH_3^-, and complexes with C=O double bonds) (Kadik et al., 2004, 2011, 2014; Mysen et al., 2009, 2011; Hirschmann, 2012; Ardia et al., 2013; Dasgupta et al., 2013; Wetzel et al., 2013; Stanley et al., 2014). These experiments were used to develop models describing the dependence of the contents of C–H–O species in planetary magmas on the redox conditions of their formation.

The separate investigation of the solubility of N–H–O and C–H–O volatiles in melts leaves unanswered the question on possible coupling of nitrogen and carbon effects on the formation of N–C–H–O molecules and complexes, in particular, on the proportions of NH_3, CH_4, and H_2O in the melts. By analogy with metallurgical systems, the solubilities of carbon and nitrogen in iron alloys are expected to be interrelated (e.g., Bouchard and Bale, 1995; Ma, 2001). In particular, the solubility of N_2 in iron alloy decreases significantly at increasing C content. Another poorly understood factor that may have a significant influence on the behavior of nitrogen and carbon in reduced magmas is the incorporation of Si in the structure of iron alloy. It results in a decrease in the solubility of carbon and nitrogen in it (e.g., Bouchard and Bale, 1995; Ma, 2001). This effect is especially important at $\Delta \log fO_2(IW) < -2$, because the Si content of iron alloy in equilibrium with silicate melt may be as high as several weight percent at such fO_2 values (e.g., Gessman et al., 2001; Ricolleau et al., 2011).

Our experimental investigations aimed at elucidating the character of simultaneous dissolution of nitrogen, carbon, and hydrogen in iron-bearing magmatic melts and equilibrium liquid iron alloy at fO_2 values two–five orders of magnitude below fO_2 (*IW*). Such extremely low fO_2 values are thought to be characteristic of the early chemical differentiation of the Earth during its melting and segregation of iron phase (e.g., Wood et al., 2006; Javoy et al., 2010; Frost et al., 2008). Despite the short duration of this period in Earth history, it probably had a profound influence on the contents of volatile components in the mantle after the completion of planetary core formation.

EXPERIMENTAL AND ANALYTICAL METHODS

Starting Materials

In order to evaluate the character of dissolution of nitrogen and its hydrogen- and oxygen-bearing compounds in the reduced mantle of the early Earth, melts of mafic–ultramafic composition should have been used; however, we selected a model FeO–Na_2O–

Table 1. Compositions of starting $NaAlSi_3O_8$ + FeO + Si_3N_4 mixtures used in the experiments, wt %

Mixture no.	Starting mixture	SiO_2	Al_2O_3	FeO	Na_2O	Si	N
L5	99%AbFeO + 1%Si_3N_4	54.4	15.4	19.8	9.4	0.6	0.4
L6	97%AbFeO + 3%Si_3N_4	53.3	15.1	19.4	9.2	1.8	1.2
L7	95%AbFeO + 5%Si_3N_4	52.2	14.8	19.0	9.0	3.0	2.0
L8	93%AbFeO + 7%Si_3N_4	51.1	14.5	18.6	8.8	4.2	2.8

AbFeO is a mixture of albite glass (80 wt %) and FeO (20 wt %).

SiO_2–Al_2O_3 melt for our study. As was previously shown (Kadik et al., 2011, 2013), silicate melts of such compositions are readily quenched to glasses. This enables the application of spectral methods for the determination of the mechanisms of dissolution of volatile components in melts at high temperatures and pressures.

The starting material for experiments was a finely dispersed mixture of albite glass $NaAlSi_3O_8$ (80 wt %) and FeO (20 wt %), which was blended with 1, 3, 5, or 7 wt % of powdered silicon nitride (Si_3N_4). The latter imposed low fO_2 values during experiments owing to the oxidation of Si_3N_4 interacting with iron-bearing silicate melt and H_2. Melting reactions at high pressures were investigated in the presence of a graphite disk, which provided conditions of system saturation with respect to free carbon. The albite glass was prepared from high-purity SiO_2 and Al_2O_3 reagents annealed before weighing at 1100°C and Na_2CO_3 dried at 200°C. An oxide mixture of the stoichiometric albite composition was ground in an agate mortar under ethanol for more than 3 h. The oxide–carbonate mixture was heated up to the temperature of Na_2CO_3 decarbonation (~900°C) at a rate of 10°C/min. Then, the temperature increased up to 1400°C, and the sample was held at this temperature for 1 h and quenched in air. The quenching rate was 100–200°C/s. At least three separate fragments of the glass were analyzed to check for its homogeneity. The glass was ground to 20 μm and stored in a desiccator until use in the experiments. The FeO powder was dried at 200°C for 24 h and added in a desired proportion to the powdered glass. The mixture was placed into an agate mortar and ground under ethanol for 3 h, after which the glass + FeO + Si_3N_4 mixture was heated to 300°C, kept at this temperature for 6 h, and stored subsequently in a desiccator. The chemical compositions of the starting mixtures are given in Table 1.

Experiments

Experiments were conducted using an anvil with hole apparatus with a working volume of 6 cm^3 at 4 GPa and 1550°C (Litvin, 1979, 1991; Kadik et al., 2013) under controlled hydrogen fugacity (Kadik et al., 2004, 2013). The experimental setup is a 2000-t uniaxial press equipped with a high-pressure system consisting of two tungsten carbide anvils with truncated cone-shaped holes. The anvils are axially aligned and separated by a pyrophyllite gasket. The resulting cavity comprises a solid-phase cell with a sample assembly. Pressure was measured at ambient temperature with an accuracy of ±0.02 GPa using Bi and Tl sensors (Kadik et al., 2013), and temperature was measured using a Pt30%Rh/Pt6%Rh thermocouple inserted radially into the center of the cell between two capsules with an accuracy of ±5°C at 1500°C and ±10°C at 1600°C. During the experiments, fH_2 was buffered through the dissociation of H_2O absorbed by fine-grained limestone or pyrophyllite outside the graphite heater up to the attainment of equal chemical potentials of H_2 in the sample and in the external solid oxygen buffer (e.g., Eugster and Wones, 1962; Kadik et al., 2004). It is assumed that fO_2 is buffered by the tungsten carbide anvils of the high-pressure system in accordance to the reaction WC + O_2 = WO_2 + C (WCWO buffer) (Taylor and Foley, 1989). The presence of traces of H_2O and the graphite heater allows us to expect the formation of a C–O–H fluid phase saturated in elemental carbon. The H_2O content of C–O–H fluid at 4 GPa, 1550°C, and fO_2 of the WCWO buffer is probably close to the maximum. The mole fraction of H_2 in the C–O–H fluid is up to 0.015, which corresponds to $\log fH_2 = 2.78$ bar.

For each experiment, 200–300 mg of the prepared mixture was loaded into a Pt capsule. To prevent interaction between Fe-bearing melt and the walls of the Pt capsule, the sample was isolated by a 0.5-mm thick W foil. The duration of experiments was 30–60 min. Quenching was performed by shutting off the power to the heater at an initial rate of 200°C/s. Oxygen fugacity in the experimental sample was controlled by a redox reaction between externally buffered hydrogen and components of Fe-bearing melt, which was reduced with the release of oxygen and metallic Fe:

$$\text{FeO (melt)} = \text{Fe (metal)} + \tfrac{1}{2}O_2. \quad (1)$$

The initial silicon nitride (Si_3N_4) is unstable under the experimental conditions and completely consumed via the oxidation reaction

$$Si_3N_4\,\text{(starting mixture)} + 3O_2 = 3SiO_2\text{(melt)} + 2N_2\text{(melt)} \quad (2)$$

and the released nitrogen reacts subsequently with the components of silicate melt and hydrogen. The redox reaction results in the attainment of the three-phase

equilibrium iron alloy + silicate melt + graphite (graphite disk in the Pt capsule). Owing to the interaction of Si_3N_4 with silicate melt and O_2 produced by FeO reduction, the fO_2 value within the Pt capsule appears to be significantly below $fO_2(IW)$. The decrease of fO_2 is proportional to the amount of Si_3N_4 in the initial mixture.

Electron Microprobe Analysis

Electron microprobe analysis was conducted at the Vernadsky Institute of Geochemistry and Analytical Chemistry, Russian Academy of Sciences using a CAMECA Camebax SX-100 instrument with four vertical spectrometers in two steps. The measurement of major elements was followed by the analysis of carbon, which required a special procedure. Carbon was measured using a PC2 pseudocrystal with 2d = 97.46 Å. In our case, the spectral peaks of carbon did not overlap with those of other measured elements, The standards for carbon were pure carbon and WC for the analysis of the metallic phase and dolomite, $CaMgCO_3$, for the silicate phase. In order to improve the statistical parameters of carbon analysis, the counting time on the peak was increased up to 30 s. The detection limit for carbon was ~0.2 wt %.

Ion Microprobe Analysis

Hydrogen was analyzed in glasses by secondary ion mass spectrometry using a CAMECA IMS-4F ion microprobe at the Yaroslavl' Filial of the Physical Technological Institute, Russian Academy of Sciences. Secondary ion beams of $^1H^+$ and $^{30}Si^+$ were used as analytical and standard signals (Smirnov et al., 1995; Sobolev and Chaussidon, 1996). To maintain charge neutrality, the sample was coated with a 20-nm Au film. The H/Si ratio of glasses was estimated using the curve of Sobolev and Chaussidon (1996), which was calibrated on the basis of the H_2O/SiO_2 (wt %) ratios of glasses containing 0.09–8.00 wt % H_2O. The processing of analytical results included the subtraction of the effect of the silicate matrix at SiO_2 contents within 49–71 wt %.

Calculation of Oxygen Fugacity

Oxygen fugacity in experiments was calculated relative to the iron–wüstite (IW) buffer equilibrium: $\Delta\log fO_2(IW) = 2\log(a_{FeO}/a_{Fe})$, where a_{FeO} is the activity of FeO in silicate melt, and a_{Fe} is the activity of Fe in liquid metallic alloy. The activities a_{FeO} and a_{Fe} were estimated from the activity coefficients γ and mole fractions x of the components, $a = x\,\gamma$, which yields $\Delta\log fO_2(IW) = 2\log(x_{FeO}/x_{Fe}) + 2\log(\gamma_{FeO}/\gamma_{Fe})$. The activity coefficient of Fe (γ_{Fe}) was taken to be one, because at Fe contents higher than ~80 wt %, its behavior in liquids is governed mainly by Raoult's law (Hultgren, 1973). Similar to the study of Kadik et al. (2014), γ_{FeO} was taken to be 1.3.

EXPERIMENTAL RESULTS

The experimental products are transparent glasses with embedded iron alloy globules 30–50 μm in size, and smaller iron alloy globules, no larger than 1–2 μm. Graphite crystals ~2–5 μm in size were occasionally observed on the surface of Fe globules (Fig. 1). The graphite disk that was used in the experiments as a source of carbon is preserved and shows sharp contacts with glass. The color of the glass varies from greenish in experiments at $\Delta\log fO_2(IW)$ from −1.4 to −2.3 to colorless in experiment at $\Delta\log fO_2(IW) = -3.0$. The spherical shape of the Fe metal phase indicates that it was liquid during the experiment. The microscopic texture of the globules resulted from quench crystallization of liquid metal during cooling (Fig. 1).

Gas inclusions were never observed in the glasses under a microscope. This indicates that melt saturation with respect to volatile compounds of nitrogen, hydrogen, and carbon with the formation of a fluid phase was not reached in the experiments.

The chemical compositions of experimental glasses show a considerable decrease in FeO content with decreasing fO_2 (Tale 2). This results from the reduction of FeO in the melt with the formation of Fe alloy in accordance with reaction (1). An increase in SiO_2 content in the melt with decreasing fO_2 is caused by the simultaneous occurrence of reactions (1) and (2), which lead to the removal of FeO from melt owing to its reduction and the addition of a certain amount SiO_2 to the melt owing to Si_3N_4 oxidation in the starting mixture. The chemical composition of the glasses and optical examination indicate complete Si_3N_4 oxidation via reaction (2). The distribution of the components of glass and metal is relatively uniform, which indicates the attainment of chemical equilibrium during the experiments.

The content of nitrogen in melt increases with decreasing fO_2 from 0.96 wt % N at $\Delta\log fO_2(IW) = -1.4$ to 4.1 wt % N at $\Delta\log fO_2(IW) = 3.0$, whereas the hydrogen content of glass is insensitive to fO_2 and lies within 0.40–0.47 wt %. The carbon content is approximately 0.3–0.5 wt %. The nitrogen content of iron alloy increases from 0.96 wt % N at $\Delta\log fO_2(IW) = -1.4$ to 6.1 wt % N at $\Delta\log fO_2(IW) = -3.0$. The carbon content decreases with decreasing fO_2 and ranges from 2.3 to 3.8 wt %.

The difference between FeO contents in $FeO–Na_2O–SiO_2–Al_2O_3$ melts and in the starting silicate mixture (20 wt %) can be used to estimate the amounts of Fe alloy and oxygen formed through melt reduction (reaction 1) and the amount of oxygen consumed for Si_3N_4 oxidation (reaction 2) (Fig. 2). These estimated indicated that the amount of oxygen produced by FeO

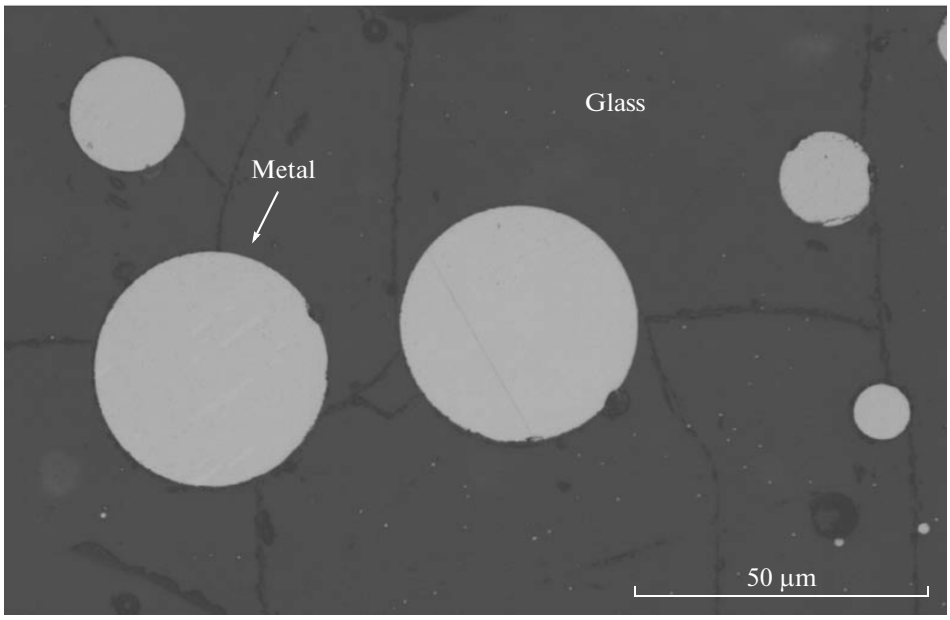

Fig. 1. Reflected-light photomicrograph of glass with metallic iron droplets and graphite crystals in the quench products of an experiment at 4 GPa, 1550°C, and $\Delta\log fO_2(IW) = -2.3$.

reduction is higher than the amount of oxygen necessary for Si oxidation with SiO_2 formation. It can be suggested that the excess oxygen corresponds to its amount consumed by the formation of nitrogen, carbon, and hydrogen species in the silicate liquid. The most important component is H_2O. Part of oxygen could be dissolved in the Fe alloy. Under the conditions of our experiments, the oxygen content of iron alloy could be as high as ~0.5 wt % (e.g., Ricolleau et al., 2011).

SOLUBILITY OF REDUCED N–H–O AND C–H–O VOLATILES IN SILICATE MELTS

One of the most remarkable features of nitrogen interaction with silicate melts is significant dependence of its solubility on fO_2 and fH_2. At fO_2 values of the modern mantle approaching the level of the fayalite–magnetite–quartz buffer, fO_2 (FMQ), nitrogen solubility in basaltic melts is rather low (less than 1 ppm) because of the molecular mechanism of N_2 dissolution in the silicate melt structure (e.g., Libourel et al., 2003). However, the nitrogen solubility increases considerably at fO_2 values below $fO_2(IW)$, and the total nitrogen content of melt may be as high as hundreds of ppm at atmospheric pressure (Libourel et al., 2003; Miyazaki et al., 2004). At high pressures and $fO_2 < fO_2(IW)$, the bulk nitrogen solubility in melt in the presence of hydrogen is up to several weight percent (Roskosz et al., 2006, 2013; Mysen et al., 2008, 2013, 2014; Mysen and Fogel, 2010; Kadik et al., 2011, 2013). The dramatic increase in nitrogen solubility is related to a change in the mechanism of its dissolution in silicate melts, which is controlled by the chemical interaction of nitrogen with hydrogen and Si–O groups with the formation of the molecular and ionic species NH_3, NH_2^-, NH_2^+, and NH_4^+.

Similar to nitrogen, carbon solubility in silicate melts depends on fO_2 and fH_2. At fO_2 values near $fO_2(FMQ)$, the dominant C–H–O species in magmas

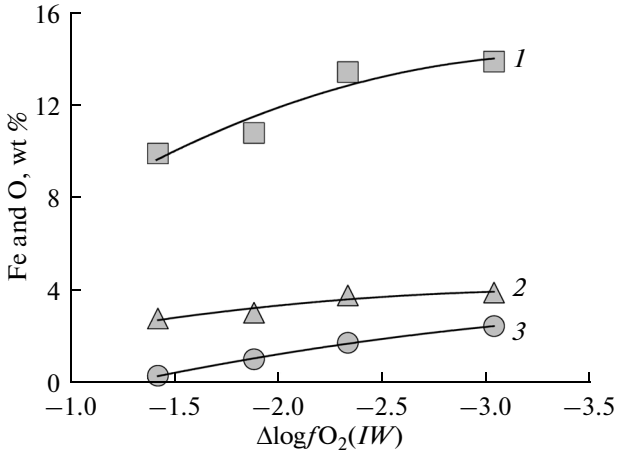

Fig. 2. Amounts of Fe and O in the $FeO–Na_2O–SiO_2–Al_2O_3$ melt during experiments in accordance with reaction (1). (*1*) Amount of Fe, (*2*) amount of O, and (*3*) amount of O consumed for Si_3N_4 oxidation in the starting mixture and SiO_2 formation via reaction (2). The difference between variants *1* and *2* corresponds to the amount of oxygen consumed by the formation of H–O complexes in melt and oxygen dissolution in liquid iron alloy.

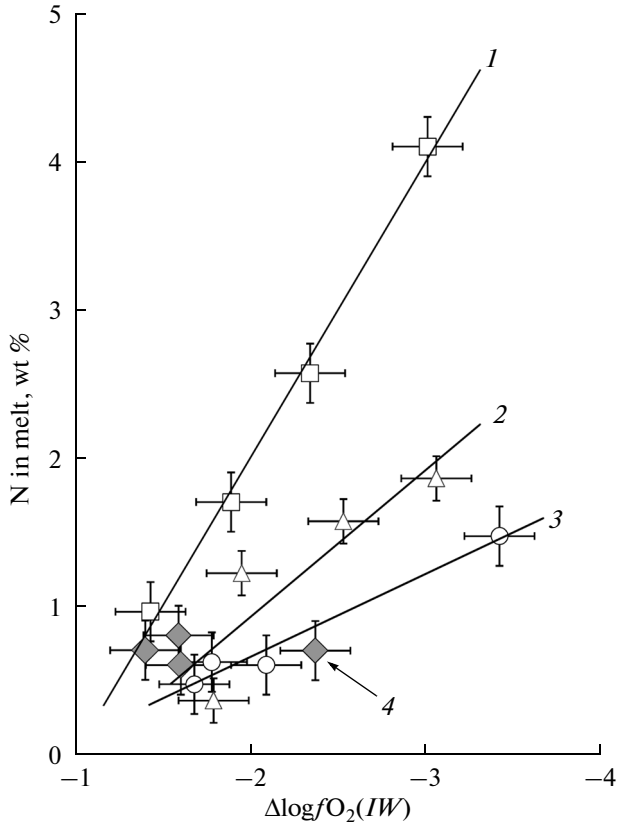

Fig. 3. Influence of fO_2 on nitrogen content in FeO–Na_2O–Al_2O_3–SiO_2 melts at the dissolution of N–C–H–O and N–H–O volatile compounds: (*1*) 4 GPa, 1550°C, melt + N–C–H–O volatile components (this study); (*2*) 4 GPa, 1550°C, melt + N–H–O volatile components (Kadik et al., 2013); (*3*) 1.5 GPa, 1400°C, melt + N–C–H–O volatile components (Kadik et al., 2011); and (*4*) model chondrite melt + N_2 at 1.8–8.2 GPa, 2500–2650 (Roskosz et al., 2013).

are CO_2 and CO_3^{2-} (e.g., Holloway, 1981; Morizet et al., 2010). At $fO_2 < fO_2(IW)$, the mechanism of carbon dissolution changes fundamentally, and the speciation of carbon in silicate melts is dominated by CH_4, CH_3, and carbonyl groups, whereas CO_2 and CO_3^{2-} occur in minor amounts (e.g., Kadik et al., 2004, 2014; Mysen et al., 2011; Mysen, 2012; Ardia et al., 2013; Dasgupta et al., 2013; Wetzel et al., 2013; Stanley et al., 2014). Compared with nitrogen, the solubility of carbon in silicate liquids at $fO_2 < fO_2(IW)$ is less significant. According to Ardia et al. (2013), Dasgupta et al. (2013), Wetzel et al. (2013), and Stanley et al. (2014), the total carbon content of basic and ultrabasic melts saturated with respect to graphite at high temperatures and pressures is tens to hundreds of ppm. The experiments of Mysen et al. (2009, 2011) and Kadik et al. (2004, 2014) at similar conditions showed somewhat higher carbon contents in model silicate melts, 0.1–0.5 wt %. This could be related to the presence of H_2O in the melt, which is believed to increase CH_4 solubility in silicate liquids (Ardia et al., 2013; Kadik et al., 2014).

The goal of our experiments was to elucidate the character of simultaneous dissolution of nitrogen and carbon in silicate liquids at $fO_2 < fO_2(IW)$.

A comparison of experimental data on the solubility of nitrogen, carbon, and hydrogen in FeO–Na_2O–SiO_2–Al_2O_3 melts at 4 GPa, 1550°C, and $fO_2 < fO_2(IW)$ with nitrogen and hydrogen solubility in the same silicate liquids under the same T–P–fO_2 conditions without carbon (Kadik et al., 2014) suggests that carbon affects nitrogen solubility in melts (Fig. 3). The total nitrogen content of melt is higher in the carbon-bearing systems. The influence of carbon on nitrogen solubility increases with decreasing fO_2. As will be shown below, the most probable reason for this is the formation of complexes in the melts with C–N bonds, the fraction of which increases with decreasing fO_2. A comparison of experimental data obtained at 4 GPa with the solubility of nitrogen and carbon in FeO–Na_2O–SiO_2–Al_2O_3 melts at a lower pressure of 1.5 GPa and 1400°C indicates the influence of pressure on reactions in the melt. In the latter case, the melts show lower nitrogen contents at the same fO_2 values (Fig. 3).

Experimental investigations of nitrogen interaction with melts of chondritic composition in the absence of hydrogen at pressures from 1 to 18 GPa and fO_2 values 1.5–2.0 orders of magnitude below $fO_2(IW)$ demonstrated that nitrogen solubility increases initially with increasing pressure but remains constant at pressures higher than ~4 GPa (Roskosz et al., 2013). At a constant fO_2 value, the solubility of nitrogen in silicate melt is pressure-independent between 4 and 15 GPa (Fig. 4). It should be noted that, at fO_2 values 1.5–2.0 orders of magnitude below $fO_2(IW)$, the solubility of nitrogen in chondrite melt is similar to that in FeO–Na_2O–SiO_2–Al_2O_3 melts (Fig. 4). However, the nitrogen solubility in FeO–Na_2O–SiO_2–Al_2O_3 melts is higher at lower fO_2 values, which is probably related to significant changes in the speciation of N–C–H–O fluids in silicate liquids.

SOLUBILITY OF N AND C IN LIQUID IRON ALLOY

Experimental studies (Kadik et al., 2011, 2013) revealed that nitrogen solubility in liquid iron alloys at high pressures and low fO_2 is 2–3 orders of magnitude higher than that in metals under ambient pressure. The solubility of nitrogen in liquid iron alloys in equilibrium with FeO–Na_2O–SiO_2–Al_2O_3 melts is 2–4 wt % at 1.5 GPa, 1400°C or 4 GPa, 1550°C, and fO_2 2–4 log units below $fO_2(IW)$ and no higher than tens of ppm at atmospheric pressure (e.g., Bouchard and Bale, 1995). The investigations of Roskosz et al. (2013) over a wide range of pressure (1–18 GPa) and fO_2 values 1.5–

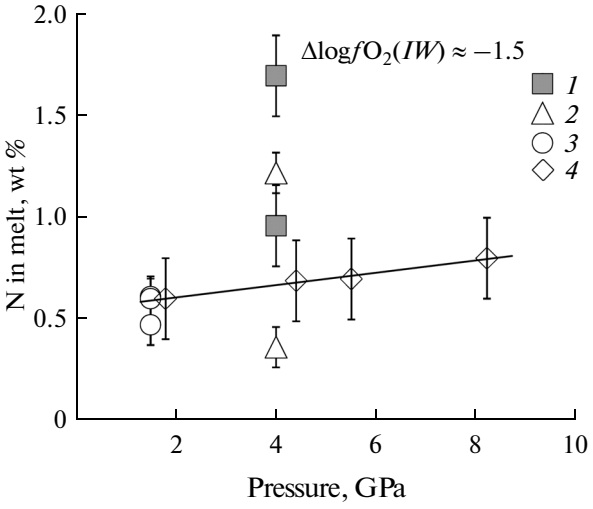

Fig. 4. Influence of pressure on the nitrogen content in $FeO–Na_2O–Al_2O_3–SiO_2$ melts and model CI chondrite melt at fO_2 1.5 orders of magnitude below $fO_2(IW)$ at the dissolution of N_2 and N–C–H–O and N–H–O volatile compounds: (*1*) 4 GPa, 1550°C, melt + N–C–H–O volatiles compounds (this study); (*2*) 4 GPa, 1550°C, melt + N–H–O volatile compounds (Kadik et al., 2013); (*3*) 1.5 GPa, 1400°C, melt + N–C–H–O volatile compounds (Kadik et al., 2011); and (*4*) model chondrite melt + N_2 at 1.8–8.2 GPa, 2500–2650 K (Roskosz et al., 2013).

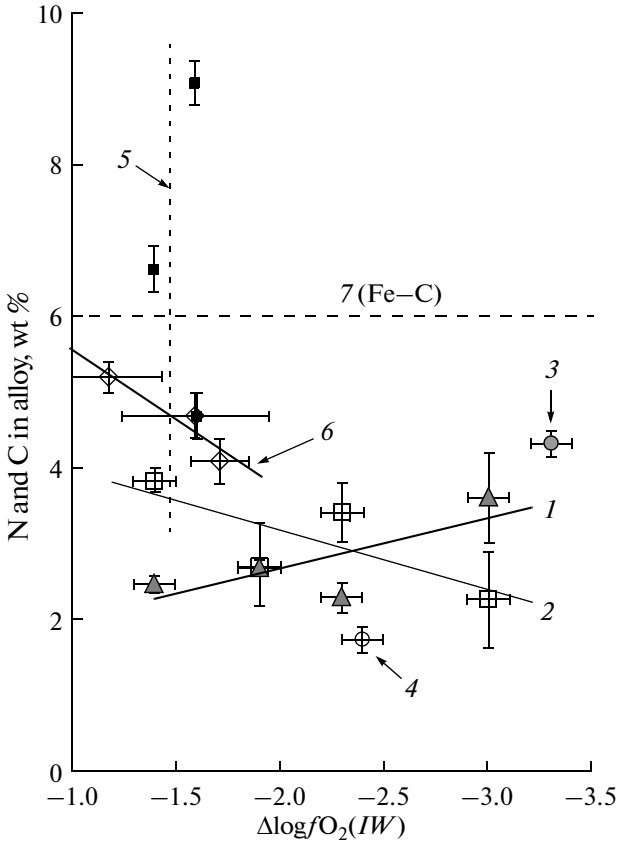

Fig. 5. Influence of fO_2 on the contents of nitrogen and carbon in liquid Fe alloy in equilibrium with $FeO–Na_2O–Al_2O_3–SiO_2$ melt: (*1*) nitrogen in N–C–Fe alloy at 4 GPa and 1550°C (this study); (*2*) carbon in N–C–Fe alloy at 4 GPa and 1550°C (this study); (*3*) nitrogen in N–Fe alloy at 4 GPa and 1550°C (Kadik et al., 2013); (*4*) nitrogen in N–C–Fe alloy at 1.5 GPa and 1400°C (Kadik et al., 2011); (*5*) nitrogen in N–Ni–Fe alloy in equilibrium with chondrite melt at 1.8, 4.4, and 8.5 GPa and 2227–2327°C (Roskosz et al., 2013); (*6*) carbon in Fe alloy at low Si content, C–Mg–Fe–Si–O system at 4 GPa and 1600°C (Takahashi et al., 2013); and (*7*) (Fe–C) carbon solubility in Fe alloy in the Fe–C system at 4 GPa and 1600°C (Wood, 1993).

2.0 orders of magnitude below $fO_2(IW)$ also indicated high nitrogen solubility in liquid iron alloys reaching 10–12% at 10–18 GPa. These authors observed a significant decrease in nitrogen solubility in FeNi alloy with increasing Ni content.

Similar to our previous results (Kadik et al., 2011, 2013), the present experiments indicate that nitrogen solubility in iron alloys at high pressures and $fO_2 < fO_2(IW)$ is high and fO_2-dependent. The nitrogen content of liquid iron alloy increases with decreasing fO_2 (Fig. 5) from 2.5% at $\Delta\log fO_2(IW) = -1.4$ to 3.6% at $\Delta\log fO_2(IW) = -3.0$. These nitrogen contents are somewhat higher than those documented in liquid iron alloys at 1.5 GPa (Kadik et al., 2011) and 4.0 GPa (Kadik et al., 2013) in equilibrium with $FeO–Na_2O–SiO_2–Al_2O_3$ melts (Fig. 4).

In general, at the same pressures and fO_2 values two orders of magnitude below $fO_2(IW)$, the nitrogen contents of liquid iron alloys observed in the present experiments and by Kadik et al. (2011, 2013) are in adequate agreement with nitrogen solubility in liquid iron alloys with low nickel contents (Roskosz et al., 2013) (Fig. 4).

The observed carbon contents in N–C–Fe alloys (2.3–3.8 wt %) are lower than the equilibrium carbon solubility in metal in the Fe–C system under the $T–P$ conditions of our experiments (~6 wt %) (e.g., Wood, 1993). A decrease in carbon solubility in liquid iron alloys was observed in the experiments of Takahashi et al. (2013), Chi et al. (2014), and Kadik et al. (2014). It is related to the incorporation of Si in the structure of the metallic phase (e.g., Bouchard and Bale, 1995). Iron alloys in equilibrium with silicate liquids at fO_2 3–4 orders of magnitude below $fO_2(IW)$ are considerably enriched in Si and depleted in C (up to negligible contents) at decreasing fO_2 (Takahashi et al., 2013; Kadik et al., 2014). Since the Si content of N–C–Fe alloys was no higher than 0.1–0.2 wt % in our experiments, it can be suggested that the decrease of carbon content was caused by the influence of nitrogen. The investigation of metallurgical systems (e.g., Bouchard and Bale, 1995) showed that nitrogen dissolution in iron alloys is accompanied by their significant depletion in carbon. Another possible factor contributing to the depression of carbon solubility is the dissolution of oxygen in N–

Table 2. Chemical compositions of glasses and iron alloy globules, wt %

Run							
glass	$\Delta\log fO_2(IW)$	SiO_2	Al_2O_3	FeO	Na_2O	N	total
854	−1.4	62.42(0.14)	12.73(0.05)	13.45(0.19)	9.94(0.18)	0.96((0.12)	99.50
855	−1.9	67.23(0.26)	13.27(0.20)	7.97(0.21)	9.93(0.19)	1.69(0.21)	99.20
856	−2.3	70.11(0.47)	13.53(0.20)	4.22(0.61)	9.23(0.80)	2.57(0.31)	99.48
857	−3.0	74.52(0.24)	13.60(0.06)	2.17(0.07)	7.56(0.10)	4.19(0.12)	102.05
Iron alloy globules							
glass	$\Delta\log fO_2(IW)$	Fe	Si	C	N	W	total
854	−1.4	92.46(0.68)	0.05(0.01)	3.83(0.16)	2.52(0.07)	0.30(0.06)	99.16
855	−1.9	93.15(0.15)	0.12(0.05)	2.71(0.56)	2.7(0.08)	0.14(0.04)	98.82
856	−2.3	92.92(0.35)	0.05(0.02)	3.43(0.38)	2.19(0.19)	0.21(15)	98.80
857	−3.0	93.06(0.19)	0.038(0.01)	2.29(0.63)	3.63(0.16)	0.10(0.07)	99.12

C–Fe alloys, the fraction of which increases in the system with increasing degree of reduction of FeO melt (Fig. 2).

INFRARED AND RAMAN SPECTROSCOPY OF N–C–H–O-BEARING GLASSES

The IR and Raman spectroscopy of experimental products (quenched glasses) was used to evaluate the mechanisms of nitrogen, carbon, and hydrogen dissolution in $FeO–Na_2O–SiO_2–Al_2O_3$ melts and the influence of oxygen fugacity, pressure, and temperature. The results of spectroscopy in the frequency range 1300–4500 cm^{-1} indicate the presence of N–H–O and C–H–O species in melts (Figs. 6a, 7a).

IR Spectroscopy

The broad asymmetric absorption feature with peaks at 3608, 3523, and 3436 cm^{-1} (Fig. 6a) is related to the stretching vibrations of hydroxyl groups (OH^-) and H_2O molecules (e.g., Stolper, 1982; Nowak and Behrens, 1995; Dianov et al., 2000; Mandeville et al., 2002). The sharp peaks at 1627–1612 cm^{-1} correspond to the bending vibrations of H_2O molecules. The weak peaks at 4543 and 4972 cm^{-1} are attributed to the stretching vibrations of OH^- and H_2O in the former case and H_2O in the latter case. The 4130 cm^{-1} weak absorption band is assigned to molecular H_2 dissolved in glass (Shelby, 1994; Schmidt et al., 1998; Plotnichenko et al., 2005).

The double absorption feature with maxima at 2330 and 2361 cm^{-1} (Fig. 6a) is interpreted as due to the stretching vibrations of C–O bonds in a CO_2 molecule dissolved in glass (e.g., Fine and Stolper, 1985; Kohn et al., 1991; Morizet et al., 2010; Mysen, 2012). The broad absorption band at ~1775–1790 cm^{-1} could associate with the stretching vibrations of the C=O double bond (Cataliotti and Jones, 1971). It should be noted that such peaks were observed in the IR spectra of C–H–O-bearing glasses obtained in experiments at $fO_2 < fO_2(IW)$ (Kadik et al., 2011, 2013, 2014). Additional investigations are necessary to identify the species with C=O bonds in the glasses.

The absorption IR bands at 1440 cm^{-1} and in the range 2800–3390 cm^{-1} are due to vibrations of bonds in N–C–H–O molecules and complexes occurring in the glass structure (Fig. 6b). It is suggested that the intense absorption peaks at 1440 and 3280 cm^{-1} and less intense peaks at 2866, 3061, and 3185 cm^{-1} are related to ammonium groups, NH_4^+, in melt. It should be noted that peaks at these frequencies were practically absent in the IR spectra of glasses produced at $\Delta\log fO_2(IW) = -3.0$, i.e., at the lowest fO_2 conditions of our experiments (Fig. 6b). The assignment of absorption at these frequencies to NH_4^+ groups is based on a comparison of the IR spectra of N–C–H–O-bearing glasses with the IR spectra of NH_4^+-bearing silicates, $NH_4AlSi_3O_8$ (hollandite), $(NH_4)_2Si_4O_9$ (wadeite), $NH_4AlSi_3O_8H_2O$ (cymrite) (Watenphul et al., 2009), and free NH_3 molecule (Herzberg, 1966) (Table 3). This inference is in agreement with the character of the IR spectra of other silicates containing NH_4^+ (micas) (Busigny et al., 2004; Harlov et al., 2001a, 2001b). The IR spectra of diopside synthesized at high pressures in the presence of nitrogen and hydrogen exhibit a strong absorption band at

Fig. 6. Infrared spectra of glasses containing N–C–O–H compounds in the ranges (a) 5000–1000 cm^{-1} and (b) 2800–3800 cm^{-1} and deconvolution of the IR spectra into separate bands. The recorded spectra were deconvoluted to Gaussian components taking into account the position and width at half-height of spectral components.

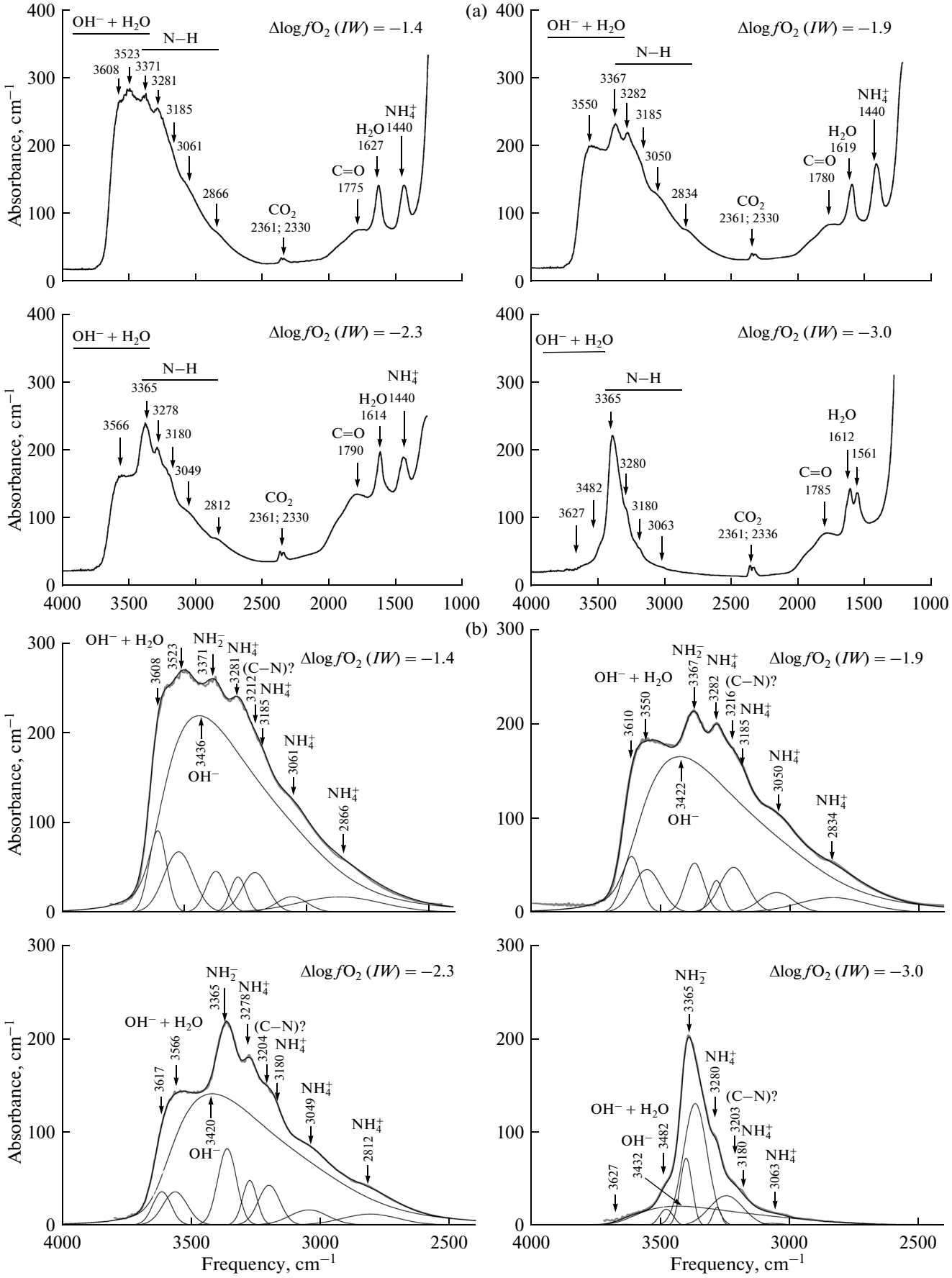
(a)
(b)
Absorbance, cm^{-1}
Frequency, cm^{-1}
$\Delta\log fO_2$ (IW) = −1.4
$\Delta\log fO_2$ (IW) = −1.9
$\Delta\log fO_2$ (IW) = −2.3
$\Delta\log fO_2$ (IW) = −3.0
OH$^-$ + H$_2$O
N–H
NH$_2^-$
NH$_4^+$
H$_2$O
C=O
CO$_2$
(C–N)?
OH$^-$
3608
3523
3371
3281
3185
3061
2866
2361; 2330
1775
1627
1440
3550
3367
3282
3050
2834
2361; 2330
1780
1619
1440
3566
3365
3278
3180
3049
2812
2361; 2330
1790
1614
1440
3627
3482
3365
3280
3180
3063
2361; 2336
1785
1612
1561
3610
3550
3367,
3282
3216
3185
3050
2834
3422
3617
3566
3365
3278
3204
3180
3049
2812
3420
3627
3432
3482
3280
3203
3180
3063

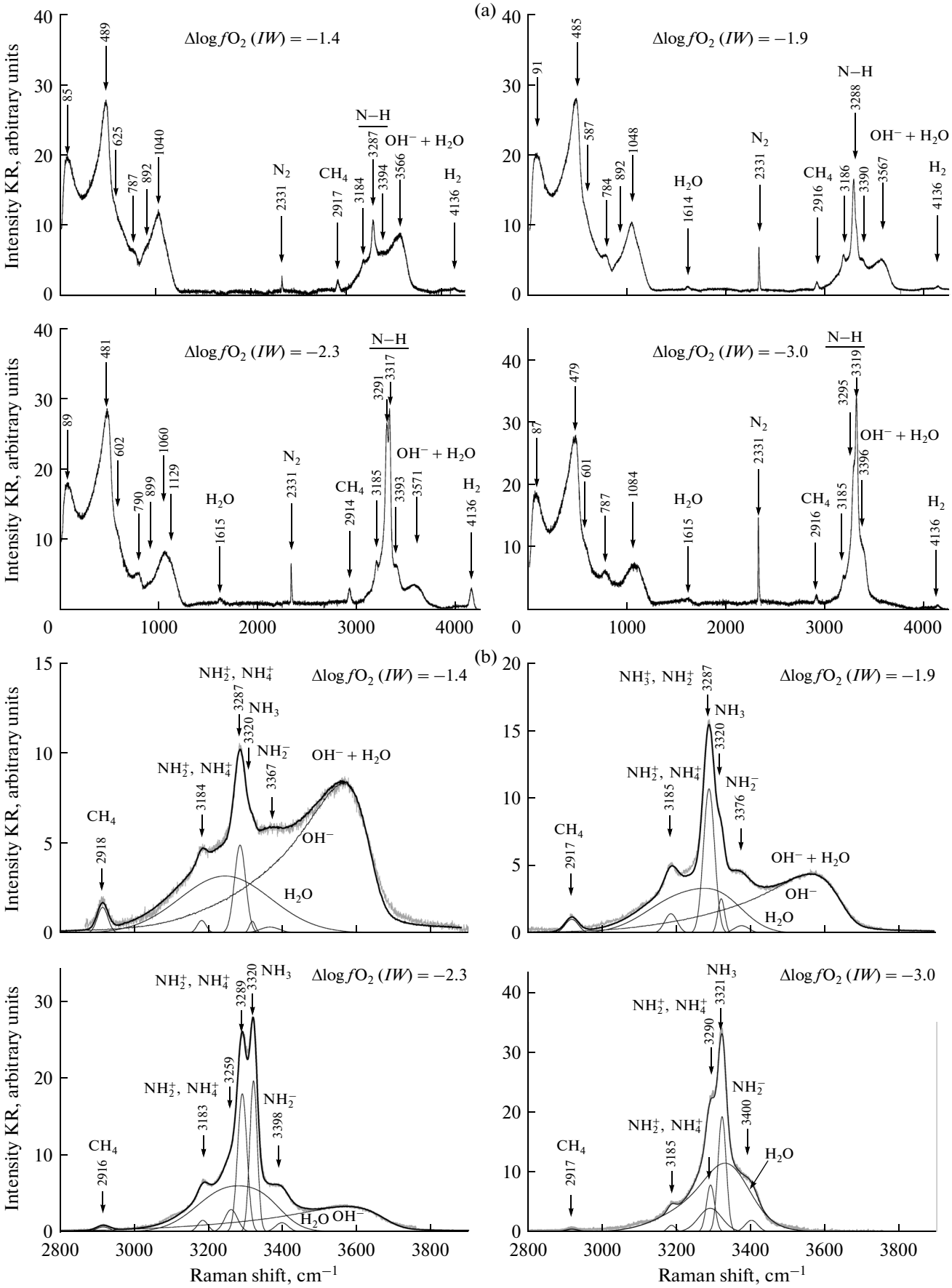
(a)
Δlog fO_2 (IW) = −1.4
Δlog fO_2 (IW) = −1.9
Δlog fO_2 (IW) = −2.3
Δlog fO_2 (IW) = −3.0
Intensity KR, arbitrary units
N–H
$OH^- + H_2O$
N_2
CH_4
H_2
H_2O
(b)
NH_2^+, NH_4^+
NH_3
NH_2^-
NH_3^+, NH_2^+
OH^-
H_2O
Raman shift, cm^{-1}

Fig. 7. Raman spectra of glasses containing N–C–O–H compounds in the ranges (a) 5000–1000 cm^{-1} and (b) 2800–3800 cm^{-1} and deconvolution of the spectra into separate bands. The recorded spectra were deconvoluted to Gaussian components taking into account the position and width at half-height of spectral components. The spectra were normalized to the 490 cm^{-1} band.

1414 cm^{-1} (Watenphul et al., 2010). It is suggested that it corresponds to the ν_4 deformation vibrations of NH_4^+ in the diopside structure.

The IR absorption peaks at 3371–3365 cm^{-1} are believed to correspond to the stretching vibrations of N–H bonds in ≡Si–NH_2 complexes, which are formed owing to nitrogen and hydrogen interaction with silicate liquid (Mysen et al., 2008).

The IR spectra of the experimental samples exhibit a weak absorption band at 3203–3216 cm^{-1} (Fig. 6b), which was not observed in our previous experiments. In this case, it can be assigned to a molecule or a complex containing both nitrogen and carbon, for instance, ≡C–NH_2 (Schrader, 1989). This problem requires further study.

Raman Spectroscopy

The Raman spectra of glasses in the range 3300–3700 cm^{-1} comprise a broad asymmetric band with maxima at 3566–3571 cm^{-1}, which are similar to those observed in the Raman spectra of hydrous glasses (e.g., Mysen and Virgo, 1986), hydrogen-bearing glasses (Luth et al., 1987), and glasses containing carbon, hydrogen, and nitrogen (Kadik et al., 2004, 2013, 2014; Mysen et al., 2008, 2009). They correspond to vibrations of O–H bonds in OH^- groups and H_2O molecules in the silicate melt structure. The weak peak at 1615 cm^{-1} is associated with bending vibrations of O–H bonds in H_2O molecules dissolved in melt. The minor band at 4136 cm^{-1} corresponds to the vibration of H–H bonds of molecular H_2 in glass (Luth et al., 1987; Plotnichenko et al., 2005).

The band centered at 2916–2918 cm^{-1} is attributed to the methane molecule, CH_4 (Socrates, 2001). A similar band was observed in the spectra of fluid inclusions in CH_4-bearing minerals (Pasteris et al., 1990; Seitz et al., 1987; Dubessy et al., 1999, 2001) and silicate melts containing carbon and hydrogen at low fO_2 (Kadik et al., 2004, 2011; Mysen et al., 2009; Mysen and Yamashita, 2010; Mysen, 2012). The broadening and displacement of this band compared to the Raman spectra of gaseous methane are due to the interaction of CH_4 molecules with the glass matrix.

According to Mysen et al. (2009, 2011) and Mysen and Yamashita (2010), the broadening of this band is related to the reaction of CH_4 with oxygen of the silicate melt network with the formation of CH_3^-(≡Si–O–CH_3) complexes, the vibrations of which are observed at the same or a similar frequency as those in methane (Socrates, 2001). However, it should be noted that in the Raman spectra of organic compounds containing CH_3 end-groups (for instance, ethane, CH_3–CH_3), two bands are observed in this range.

Table 3. Frequencies of IR absorption bands of NH_4^+-bearing silicates assigned to different vibration modes (ν, cm^{-1}) according to Watenphul et al. (2009) compared with the IR spectral characteristics of nitrogen-bearing glasses (this study)

ν (cm^{-1})	$(NH_4)^+$	NH_4-*Hld*	NH_4-*SWd*	NH_4 *Cym*	NCHO-melt
ν_4	1397	1402 sh (m)	1397 sh (m)	1404 sh (w)	
		1436 (s)	1422 (s)	1423 (s)	1438 (s)
		1459 sh (m)	1438 sh (m)	1447 sh (m)	
ν_2	1685	1669 (w)	1671 (w)		
$2\nu_4$		2878 (m)	2842 (m)	2852 (w)	2866 (m)
$\nu_2 + \nu_4$		3043 (m)	2967 sh (m)	3091 sh (m)	3061 (m)
			3025 (m)		
$2\nu_2$		3140 (s)	3140 (s)	3179 sh (m)	3185 (m)
ν_3	3134	3223 (m)	3320 (m)	3233 sh (m)	
		3281 sh (w)		3294 (s)	3285 (s)
		3333 sh (w)			

$(NH_4)^+$ denotes the values for free NH_4^+ according to Herzberg (1966); values for hollandite (*Hld*, $NH_4AlSi_3O_8$), Si-wadeite (*SWd*, $(NH_4)_2Si_4O_9$), and cymrite (*Cym*, $NH_4AlSi_3O_8H_2O$) are after Watenphul et al. (2009); NCHO-melt is the results of this study; intensities of bands: *sh*, band shoulder in the spectrum; *w*, weak; *m*, medium; and *s*, strong.

The strong narrow peak at 2331 cm^{-1} corresponds to molecular nitrogen dissolved in glass. At normal temperature and pressure, the vibration of N_2 molecules in gas is observed at 2335 cm^{-1} (e.g., Lofithus and Krupnie, 1977). A similar peak of N_2 in glass was documented by Roskosz et al. (2006), Mysen et al. (2008), Mysen and Fogel (2010), and Kadik et al. (2011, 2013), who studied the solubility of nitrogen and its compounds in silicate melts at high pressures.

The Raman spectra of glasses display intense peaks at 3287–3295 and 3320 cm^{-1}, as well as peaks at 3185 and 3387–3390 cm^{-1} (Fig. 7b) occurring in the frequency region corresponding to bond vibrations in N–H–O species (e.g., Dickinson et al., 1929; Yeo and Ford, 1994; Kowal, 2002). Their possible nature in N–H-bearing silicate melts under reduced conditions were investigated by Roskosz et al. (2006), Mysen et al. (2008, 2010), and Kadik et al. (2013). The peak at 3320 cm^{-1} is similar to that observed in the Raman spectra of gaseous NH_3 molecules (Dickinson et al., 1929; Wang et al., 1973; Durig et al., 1989). The Raman band at 3287–3295 cm^{-1} corresponds to N–H vibrations of the amine group NH_2^- ($\equiv Si-NH_2$) (e.g., Socrates, 2001), which is produced by the chemical interaction of nitrogen and hydrogen with silicate melts (Mysen et al., 2008). The band around 3288 cm^{-1} probably associates with the N–H vibrations of a modified hydrogen bond in the NH_3 molecule (Yeo and Ford, 1994), and the bands at 3185 cm^{-1} are related to the vibrations ofNH_2^+ ($\equiv Si-O-NH_2$) (Mysen et al., 2008). It is thought that the $\equiv Si-O-NH_2$ complexes are also products of chemical interaction of nitrogen and hydrogen with silicate melt. However, the Raman peaks at 3288 and 3185 cm^{-1} can be interpreted as resulting from the vibration of bonds inNH_4^+, which was suggested based on the IR spectra of the same glasses. We do not exclude the possibility of a different interpretation of bands at 3185, 3290, and 3390 cm^{-1} in the Raman spectra of glasses. They could associate with the $2\nu_4$, ν_1, and ν_3 vibrations in the NH_3 molecule, which can be inferred from the comparison with the spectra of ammonium (Nakamoto, 1978).

COMPARISON WITH PREVIOUS WORK

The IR and Raman spectroscopy of the glasses showed that the dissolution of N–C–O–H volatiles in $FeO-Na_2O-SiO_2-Al_2O_3$ melts in equilibrium with liquid iron alloy and graphite at 4 GPa, 1550°C, and fO_2 values 2–4 orders of magnitude below $fO_2(IW)$ is accompanied by the formation of NH_3, N_2, and CH_4 molecules and $\equiv Si-NH_2$, $\equiv Si-O-NH_2$, and NH_4^+ complexes. The melts contain very minor amounts of CO_3^{2-}. This is consistent with the estimates of the influence of fO_2 on the stability of CO_3^{2-} in magmatic melts (Hirschmann and Withers, 2008; Stanley et al., 2014), which indicated very low CO_3^{2-} contents in silicate liquids at fO_2 values two orders of magnitude below $fO_2(IW)$. In addition to compounds with nitrogen and carbon, dissolved hydrogen exists in melt as H_2 and H_2O molecules and hydroxyl groups, OH^-. The volatile N–C–O–H species in $FeO-Na_2O-SiO_2-Al_2O_3$ melts in equilibrium with liquid iron alloy and graphite are in general identical to those observed during nitrogen and carbon dissolution in iron-free binary silicate melts of alkaline and calc-alkaline composition (Mysen et al., 2008; Mysen and Yamashita, 2010; Mysen and Fogel, 2010), Fe-bearing aluminosilicate melt (Kadik et al., 2010, 2013, 2014), and basic melts (Kadik et al., 2004; Dasgupta et al., 2013; Ardia et al., 2013; Wetzel et al., 2013). In contrast to the results for basaltic melts (Wetzel et al., 2013; Stanley et al., 2014), the $FeO-Na_2O-SiO_2-Al_2O_3$ glasses do not show a band at 2110 cm^{-1} in Raman spectra (Wetzel et al., 2013) and a band at 2205 cm^{-1} in IR spectra (Stanley et al., 2014); these bands associate with the formation of complexes with C=O bonds in basaltic liquids. The vibrations at 2110 cm^{-1} in the Raman spectra and at 2205 cm^{-1} in IR spectra were assigned to the $Fe(CO)_5$ and $Fe(CO)_6^{2+}$, respectively. It is conceivable that the absence of these species in the $FeO-Na_2O-SiO_2-Al_2O_3$ melts was due to the lower fO_2 values in our experiments compared with those of Wetzel et al. (2013) and Stanley et al. (2014). In the former case, fO_2 was 2–4 orders of magnitude below $fO_2(IW)$, and, in the later case, fO_2 values are close to or 1–2 orders of magnitude higher than $fO_2(IW)$. On the other hand, it is possible that complexes with C=O double bonds are formed in the $FeO-Na_2O-SiO_2-Al_2O_3$ melts at $fO_2 < fO_2(IW)$, but their nature is probably different and poorly known. Their formation in melts is supported by IR absorption bands at 1775–1785 cm^{-1} in the $FeO-Na_2O-SiO_2-Al_2O_3$ glasses (Fig. 6a). The formation of complexes with C=O double bonds in silicate liquids at $fO_2 < fO_2(IW)$ was established by Kadik et al. (2011, 2013).

The determination of nitrogen and hydrogen solubility in $FeO-Na_2O-SiO_2-Al_2O_3$ melts both in the absence (Kadik et al., 2013) and in the presence of free carbon (graphite) in the system (this study) implies the presence of generally similar N–H–O molecules and complexes at 4 GPa, 1550°C, and $fO_2 < fO_2(IW)$. An exception is an absorption band in the IR spectra of the glasses at 3203–3216 cm^{-1}, which appears in silicate liquids saturated in carbon and nitrogen.

INFLUENCE OF fO_2 ON THE FORMATION OF N–C–O–H SPECIES IN MELT

Figures 8 and 9 show the normalized spectral characteristics of glasses, Abs/Abs_0 and I/I_0, where Abs_0 is the absorption coefficient for a band of the IR spectra and I_0 is the coefficient of the integral intensity of

Raman bands at $\Delta\log fO_2(IW) = -1.4$. The degree of silicate melt polymerization is characterized in these diagrams by the NBO/T ratio (Mysen, 2012), where NBO is the number of nonbridging oxygens, and T is the number of tetrahedral cations. A decrease in NBO/T corresponds to an increase in the degree of silicate melt polymerization.

Variations in I/I_0 and Abs/Abs_0 of the Raman and IR spectra of the glasses indicate an increase in the content of the reduced nitrogen species $\equiv Si-NH_2$ and $\equiv Si-O-NH_2$ at decreasing fO_2 (Figs. 8b, 9b). The proportion of the integral intensities of the 3320 and 3385 cm^{-1} bands shows that the content of molecular NH_3 increases sharply relative to that of $\equiv Si-NH_2$. At fO_2 values 2–3 orders of magnitude below $fO_2(IW)$, the reduction of nitrogen is accompanied by a considerable decrease in the contents of $\equiv Si-O-NH_2$ and NH_4^+ species (Figs. 8a, 9a). Hence, it can be suggested that NH_3 molecules become the dominant nitrogen species in melts at low fO_2. Despite the low fO_2 values, molecular N_2 is present in the melt, and its amount increases with decreasing fO_2 and NBO/T (Fig. 8b). The intensity of the 2331 cm^{-1} band in the Raman spectra indicates that the total content of molecular nitrogen in melts is not high.

According to the interpretation of Mysen and Fogel (2010) and Mysen (2013), the formation of $\equiv Si-NH_2$ complexes is controlled by the chemical interaction of NH_3 with the silicate melt matrix, which results in the appearance of $Si-NH_2$ and Si–OH bonds through the reaction:

$$\equiv Si-O-Si\equiv + NH_3 \leftrightarrow \equiv Si-NH_2 + HO-Si\equiv, \quad (3)$$

where $\equiv Si-O-Si\equiv$ denotes a bridging oxygen in the glass matrix, and $Si-NH_2$ and Si–OH are the formed end-groups. The interaction of NH_3 with the silicate melt matrix is similar to H_2O dissolution with the for-

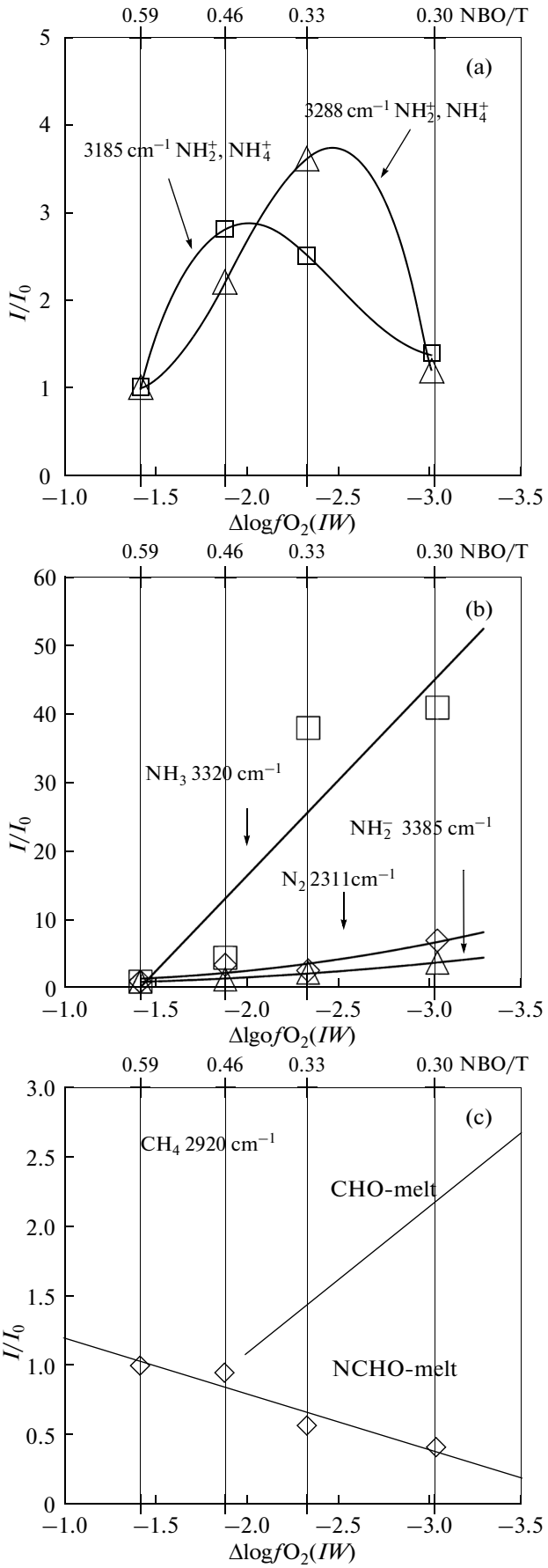

Fig. 8. Variations in the I/I_0 ratio of the Raman spectra of glasses characterizing the influence of fO_2 on the proportions of N–C–O–H species in $FeO-Na_2O-Al_2O_3-SiO_2$ melts at 4 GPa and 1550°C. I_0 is the integral intensity of Raman bands at $\Delta\log fO_2(IW) = -1.4$.

I/I_0 values are given for the Raman bands of (a) NH_2^+, NH_4^+ (3185 cm^{-1}) and NH_2^+, NH_4^+ (3288 cm^{-1}); (b) NH_3 (3320 cm^{-1}), NH_2^- (3385 cm^{-1}), and N_2 (2331 cm^{-1}); and (c) CH_4 (2917 cm^{-1}) according to this study (NCHO-melt) and Kadik et al. (2014) (CHO-melt) and H_2 (4136 cm^{-1}). The NBO/T values of melts are given accounting for the total content of H_2O in 14 glasses determined by IR spectroscopy: 0.59 (0.18), 0.46 (0.14), 0.33 (0.06), and 0.30 (0.04) corresponding to experimental fO_2 values. Values in parentheses are NBO/T values ignoring the H_2O content of glasses.

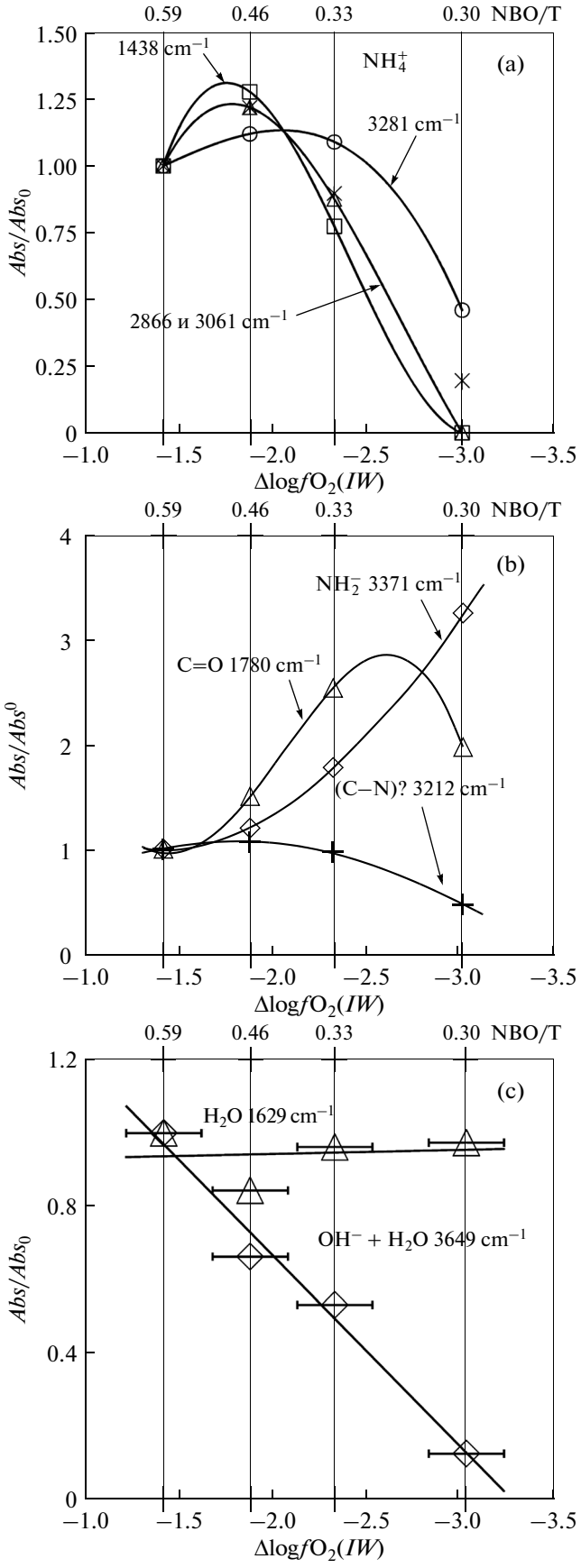

Fig. 9. Variations in the Abs/Abs_0 ratio of the IR spectra of glasses characterizing the influence of fO_2 on the proportions of N–C–O–H species in $FeO–Na_2O–Al_2O_3–SiO_2$ melts at 4 GPa and 1550°C. Abs_0 is the absorption coefficients of IR bands at $\Delta\log fO_2(IW) = -1.4$.

Abs/Abs_0 values are given for the IR bands of (a) NH_4^+ (1438, 2688, 30161, and 3281 cm^{-1}); (b) NH_2^- (3371 cm^{-1}), (C–N)? (3212 cm^{-1}), and C=O (1780 cm^{-1}); and (c) OH^- (3549 cm^{-1}) and H_2O (1629 cm^{-1}). See Fig. 8 for the determination of NBO/T values.

mation of hydroxyl groups, OH^- (e.g., Mysen and Virgo, 1986; Kohn et al., 1991):

$$\equiv Si–O–Si\equiv (melt) + H_2O \longleftrightarrow \equiv Si–H\ (melt) + H–O–Si\equiv (melt). \quad (4)$$

The stronger changes in the integral intensity of the Raman band at 3320 cm^{-1} (NH_3) compared with the 3385 cm^{-1} band ($\equiv Si–NH_2$) indicate an increase in $NH_3/\equiv Si–NH_2$ content with decreasing fO_2 and NBO/T (Fig. 8b). However, according to reaction (3), a decrease in melt NBO/T, i.e., the formation of silicate melts with higher bridging oxygen contents, should have decreased the NH_3/NH_2^- ratio, which was not the case in our experiments. Therefore, it can be suggested that fO_2 plays a dominant role in the formation of NH_3 and $\equiv Si–NH_2$ in the melt through redox reactions involving simultaneously nitrogen, carbon, hydrogen, and oxygen.

It is believed that, similar to noble gases, the N_2, NH_3, and CH_4 molecules reside in structural cavities of silicate liquids (Carroll and Webster, 1994; Mysen and Richet, 2005, ch. 16). This is indicated by the increasing solubility of N_2, NH_3, and CH_4 with increasing degree of silicate melt polymerization and, correspondingly, increasing number of sites suitable for these molecules in the silicate liquid matrix (Mysen et al., 2011; Dasgupta et al., 2013). Within this model, the increase in N_2 and NH_3 contents in $FeO–Na_2O–SiO_2–Al_2O_3$ melts with decreasing fO_2 can be attributed to an increase in the degree of silicate melt polymerization induced by FeO reduction. On the other hand, the CH_4 content decreases with decreasing NBO/T. Similar to the case of the formation of N–H bonds, this may indicate that a change in the melt structure accompanying its polymerization is not the only factor of CH_4 dissolution.

The Abs/Abs_0 values that are assigned to complexes with C=O double bonds increase sharply with decreasing fO_2 and reach maxima at around $\Delta\log fO_2(IW) = -3$ (Fig. 8c). A further fO_2 decrease is accompanied by a decrease in Abs/Abs_0. The existence of a maximum in the fO_2 dependence of the content of complexes with C=O double bonds suggests that these complexes react

with other C–O–H species in melt at fO_2 values in the system below $\Delta\log fO_2(IW) = -1.4$.

The observed Abs/Abs_0 values indicate that a decrease in fO_2 is accompanied by the occurrence of redox reactions resulting in a significant decrease in the content of OH^- groups in melt at minor variations in molecular H_2O content (Fig. 9c) and, correspondingly, a decrease in OH^-/H_2O. The fO_2 dependence of I/I_0 for H_2 displays a sharp maximum and a significant decrease below $\Delta\log fO_2 \approx -2.5$. This tendency for H_2 deserves further experimental investigations. Owing to the high diffusion mobility of hydrogen molecules in glasses, part of hydrogen could be lost from the glasses after the completion of melting experiments at high pressures and temperatures. However, there is evidence that the diffusive loss of hydrogen from glasses is not significant, if at all. This is supported by observations of hydrogen contents in glasses obtained by quenching carbon- and water-bearing melts (Hirschmann et al., 2012), which did not change during the prolonged storage of the glasses after the experiments.

H_2O CONTENT IN MELTS

Total water contents ($OH^- + H_2O$) in glasses were determined on the basis of the Bouguer–Lambert–Beer law using Abs_{3548} values from the IR spectra in the region of ($OH^- + H_2O$) vibrations at 3548 cm^{-1} (e.g., Mercier et al., 2010). The molar extinction coefficient, ε_{3548}, was estimated from its dependence on glass NBO/T calibrated by Mercier et al. (2010). The obtained ($OH^- + H_2O$) contents recalculated to H_2O are 2.93, 1.98, 1.65, and 0.41 wt % at $\Delta\log fO_2(IW)$ values of –1.4, –1.8, –2.3, and –3.0, respectively. The high H_2O contents result from the character of redox reactions in our experiments. They are related to FeO reduction in the melts via reaction (1) with release of considerable amounts of oxygen (Fig. 3), which contributes to the formation of oxidized carbon and hydrogen species at the given fH_2 value. These include complexes with C=O double bonds, OH^- groups, and H_2O molecules. The formation of OH^- groups could be additionally related to the interaction of molecular NH_3 with the silicate melt matrix via reaction (4), which was discussed by Mysen et al. (2013, 2014). Similarly, OH^- groups may be produced by the interaction of molecular CH_4 with silicate melts (Kadik et al., 2014):

$$\begin{aligned} &\text{Si–O–Si (melt)} + CH_4 \\ &= \text{Si–O–CH}_3\text{ (melt)} + \text{H–O–Si (melt)}. \end{aligned} \quad (5)$$

Thus, the experiments suggest that OH^- groups and molecular H_2O can be stable in silicate liquids at certain fO_2 values below $fO_2(IW)$.

NITROGEN DEGASSING DURING MELTING OF THE EARTH'S EARLY REDUCED MANTLE

The investigation of the nature of redox reactions of nitrogen, carbon, and hydrogen with $FeO–Na_2O–Al_2O_3–SiO_2$ melts and liquid iron alloys at 4 GPa, 1550°C, and fO_2 values 1.5–3 orders of magnitude below $fO_2(IW)$ has a number of important implications for the estimation of conditions under which volatile nitrogen compounds formed during the melting of the Earth's early reduced mantle.

According to estimates (Marty, 1995; Javoy, 1997; Cartingy et al., 2001), the Earth's mantle contains between 2 and 40 ppm nitrogen. The solubility of nitrogen in silicate melts at high pressure and $fO_2 < fO_2(IW)$ is much higher. Therefore, it is reasonable to assume that most of terrestrial nitrogen was initially dissolved in the magma ocean (e.g., Li et al., 2013). Its further behavior during the evolution of the early reduced mantle had to be controlled by nitrogen partitioning between silicate melt, metallic phase, and products of magma ocean crystallization and degassing. Experimental studies (Mysen et al., 2008, 2013, 2014; Mysen and Fogel, 2010; Kadik et al., 2011, 2013; Roskosz et al., 2013; Li et al., 2013, 2015; Li and Keppler, 2014) have demonstrated the possible occurrence of such partitioning during the early geochemical history of the Earth.

If the nitrogen content of the material from which the Earth was formed was similar to the nitrogen abundance in chondrites, ~1100 ppm (Keridge, 1985; Javoy, 1997; Marty, 2012), either more than 95% of primordial nitrogen had to be lost from the Earth to space during accretion or a significant amount of nitrogen should still be retained in the Earth's interiors (e.g., Marty, 2012). The relative abundance of nitrogen compared with other gases in the present-day atmosphere (Marty, 2012) suggests that the nitrogen loss to space, if occurred, could not be considerable. This motivated searches for silicate and metallic phases, either liquid or crystalline, in the mantle that could account for the burial of nitrogen in the planetary interiors.

This study confirmed the conclusions of Kadik et al. (2011, 2013) and Roskosz et al. (2013) on high nitrogen solubility in iron alloys at high pressures and $fO_2 < fO_2(IW)$. It increases with increasing pressure and hydrogen content and decreasing fO_2. The nitrogen content of iron alloy may be as high as 4–6 wt % at 1.5–5 GPa and up to ~10 wt % at 9–12 GPa (Roskosz et al., 2013). Thus, nitrogen exhibits siderophile behavior under the conditions of magma ocean formation at $fO_2 < fO_2(IW)$. This implies that part of nitrogen could be dissolved in iron alloys segregating from the melting products of the early reduced mantle and buried subsequently in the Earth's metallic core.

The experimental results of Watenphul et al. (2010) and Li et al. (2013) allow us to suggest that nitrogen

could be dissolved in the crystallization products of the magma ocean and, thus, be retained in the minerals of the Earth's early mantle. Nitrogen solubility in forsterite, pyroxenes, and pyrope at 15–35 kbar is between 3 and 100 ppm; it increases with decreasing fO_2 and is controlled by the formation of ammonium cation (NH_4^+) in the crystals. It should be noted that, according to our experiments, a similar mechanism of nitrogen dissolution is characteristic of $FeO–Na_2O–Al_2O_3–SiO_2$ melts; however, it appeared that the stability of NH_4^+ is significantly dependent on fO_2. At 4 GPa and fO_2 values 2.5–3.0 orders of magnitude lower than $fO_2(IW)$, nitrogen dissolution in aluminosilicate liquids does not result in the formation of NH_4^+. If this tendency will also prove to be valid for crystals, nitrogen burial in the products of magma ocean crystallization will be restricted to fO_2 values 2.5–3.0 orders of magnitude below $fO_2(IW)$.

The nitrogen solubility in silicate melts and mantle crystalline phases decreases with increasing fO_2 (Li et al., 2013). Therefore, it can be supposed that an increase in fO_2 during the chemical differentiation of the Earth's early reduced mantle could cause short-term intense nitrogen release from deep magmas and crystalline phases. The investigations of Galimov (2005), Wood et al. (2006), Corgne et al. (2008), and Javoy et al. (2010) suggested that an increase in fO_2 in the deep parts of the early mantle and magma ocean could be related to the self-oxidation of planetary material owing to the redistribution of Fe, Si, and O between silicate and metallic phases. According to Galimov (2005), reduced conditions were characteristic of the mantle during the initial stage of the formation of the Earth's core. The next evolutionary stage involved interaction between the silicate mantle and the metallic core: $3Fe^{2+}O$ (mantle) $\rightarrow Fe^0$ (core) + $Fe_2^{3+}O_3$(mantle), which was accompanied by an increase in fO_2 in the planetary interiors, probably up to the high fO_2 values that are observed in the upper mantle. According to estimates, this stage could last 150–300 Myr. The model of heterogeneous accretion (Rubie et al., 2011) postulates an increase in fO_2 with increasing mass of the growing planet within the $\Delta\log fO_2(IW)$ range from –5 to –2. The increase in fO_2 in the deep parts of the Earth's early mantle could be caused by Si transfer owing to interaction between the silicate mantle and metallic core: SiO_2(silicate) + 2Fe (metal) = Si (metal) + 2FeO (silicate) (Frost et al., 2008; Javoy et al., 2010). The incorporation of Si in the core increased the abundance of FeO in the mantle, which became progressively oxidized as $\Delta\log fO_2(IW)$ increased supposedly from –4.5 to –1.5. It is assumed that fO_2 increased in the magma ocean owing to FeO disproportionation during $(Mg,Fe,Al)(Al,Si)O_3$ perovskite crystallization via the reaction $3Fe^{2+}O$ (melt) + Al_2O_3 (melt) = $2Fe^{3+}AlO_3$ (perovskite) + Fe^0 (metal) (Frost et al., 2008; Wood et al., 2006). The precipitation of a metallic phase was accompanied the gradual oxidation of the magma ocean and a $\Delta\log fO_2(IW)$ increase from –5 to –2. According to the experiments reported here and recent data of Kadik et al. (2011, 2013) and Roskosz et al. (2013), this region of fO_2 values corresponds to conditions under which the supposed initial nitrogen content in the Earth's early mantle could be completely dissolved in the equilibrium melt and metallic phases. The degassing of such melts with dissolved nitrogen would require a more significant increase in fO_2 in the zones of early mantle melting up to the condition $fO_2 > fO_2(IW)$.

Such conditions were probably reached in the upper parts of the magma ocean owing to fO_2 stratification with depth (Hirschmann et al., 2012). The distribution of fO_2 with depth is controlled by the influence of pressure, temperature, and convective mixing of melts in the ocean on the Fe_3^+/Fe_2^+ ratio and fO_2 in silicate liquid and, correspondingly, on the behavior of volatile components. It is also possible that the stratification resulted from the self-oxidation of melts at their low-pressure degassing owing to the release of reduced N–C–H–O species from the melts. This process had to result in an increase in fO_2 owing to changes in the proportions of oxidized and reduced compounds of nitrogen, carbon, hydrogen, and oxygen in the melt. This is supported by the experimental results of Holloway and Jakobsson (1986), who studied equilibria between silicate melts, graphite, and C–O–H volatile compounds at high temperatures and pressures and $fO_2 = fO_2(IW)$. They showed that the formation of fluids enriched in CH_4, CO, and H_2 results in a significant increase in the fraction of oxygen-rich C–O–H species in the melt, primarily, H_2O. The fractional degassing of reduced gaseous components will enhance this effect resulting in an additional increase in fO_2 (Kadik and Lukanin, 1986).

Shallow local magmatic degassing at the contact with the early atmosphere could be sustained by the convective transport of dissolved volatile components from the deep levels of the magma ocean. It could also be enhanced by the directional crystallization of the magma ocean, which is suggested by the model of Elkins-Tanton (2008).

ACKNOWLEDGMENTS

We are grateful to Yu.A. Litvin for the helpful discussion of the manuscript and assistance in high-pressure experiments.

This study was financially supported by the Russian Foundation for Basic Research, project no. 14-05-00136a, and Program 28 of the Presidium of the Russian Academy of Sciences "Origin and Evolution of Life in the Solar System: from Cosmochemistry to Biochemistry".

REFERENCES

J. F. Adler and Q. Williams, "A high-pressure X-ray diffraction study of iron nitrides: implications for Earth's core," J. Geophys. Res. **110**, B01203 (2005). doi: 10.1029/2004JB003103

P. Ardia, M. M. Hirschmann, A. C. Withers, and B. D. Stanley, "Solubility of CH_4 in a synthetic basaltic melt, with applications to atmosphere–magma ocean–core partitioning of volatiles and to the evolution of the Martian atmosphere," Geochim. Cosmochim. Acta **114**, 52–71 (2013).

D. Bouchard and C. W. Bale, "Simultaneous optimization of thermodynamical data for liquid iron alloys containing C, N, Ti, Si, Mn, Si, and P," Metall. Trans. B **26B**, 467–483 (1995).

V. Busigny, P. Cartigny, P. Philippot, and M. Javoy, "Quantitative analysis of ammonium in biotite using infrared spectroscopy," Am. Mineral. **89**, 1625–1630 (2004).

M. R. Carroll and J. D. Webster, "Solubilities of sulfur, noble gases, nitrogen, chlorine, and fluorine in magmas," in *Volatiles in Magmas*, Ed. by M. R. Carroll and J. R. Holloway, Rev. Mineral. **30**, 231–279 (1994).

P. Cartigny, F. Jendrzejewski, F. Pineau, E. Petit, and M. Javoy, "Volatile (C, N, Ar) variability in MORB and the respective roles of mantle source heterogeneity and degassing: the case of the Southwest Indian Ridge," Earth Planet. Sci. Lett. **194**, 241–257 (2001).

R. Cataliotti and R. N. Jones, "Further evidence of Fermi resonance in the C–O stretching band of cyclopentanone," Spectrochim. Acta **27a**, 2011–2013 (1971).

D. C. Catling and M.W. Claire, "How Earth's atmosphere evolved to an oxic state: a status report," Earth Planet. Sci. Lett. **237**, 1–20 (2005).

Y. Chi, R. Dasgupta, M. S. Duncan, and N. Shimizu, "Partitioning of carbon between Fe-rich alloy melt and silicate melt in a magma ocean—implications for the abundance and origin of volatiles in Earth, Mars, and the Moon," Geochim. Cosmochim. Acta **139**, 447–471 (2014).

A. Corgne, S. Keshav, B. J. Wood, W. F. McDonough, and Y. W. Fei, "Metal–silicate partitioning and constraints on core composition and oxygen fugacity during Earth accretion," Geochim. Cosmochim. Acta **72**, 574–589 (2008).

R. Dasgupta, H. Chi, N. Shimizu, A. S. Buono, and D. Walker, "Carbon solution and partitioning between metallic and silicate melts in a shallow magma ocean: implications for the origin and distribution of terrestrial carbon," Geochim. Cosmochim. Acta **102**, 191–212 (2013).

E. M. Dianov, M. M. Bubnov, A. N. Gurianov, V. F. Hopin, E. B. Kryukova, V. G. Plotnichenko, A. A. Rybaltovskii, and V. O. Sokolov, "Phosphosilicate glass optical fibers—a promissing material for Raman lasers," Proc. ECOC 2000, Sept. 3–7, Munich, Germany **3**, 135–136 (2000).

R. G. Dickinson, R. T. Dillon, and F. Raseti, "Raman spectra of polyatomic gases. Phys. Rev. **B 34**, 582–589 (1929).

J. Dubessy, A. Moissette, R. J. Bakker, J. D. Frantz, and Y. G. Zhang, "High-temperature Raman spectroscopic study of H_2O–CO_2–CH_4 mixtures in synthetic fluid inclusions; first insights on molecular interactions and analytical implications," Eur. J. Mineral. **11**, 23–32 (1999).

J. Dubessy, S. Buschaert, W. Lamb, J. Pironon, and R. Thiery "Methane-bearing aqueous fluid inclusions; Raman analysis, thermodynamic modeling and application to petroleum basins," Chem. Geol. **173**, 193–205 (2001).

J. R. Durig, W. B. Beshir, S. E. Godbey, and T. J. Hizer, "Raman and infrared spectra, conformational stability and ab initio calculations for n-propylamine," J. Raman Spectroscopy **20**, 311–333 (1989).

L. T. Elkins-Tanton, "Linked magma ocean solidification and atmospheric growth for Earth and Mars," Earth Planet. Sci. Lett. 271(1–4), 181–191 (2008).

H. P. Eugster and D. R. Wones, "Stability relations of the ferruginous biotite, annite," J. Petrol. **3**, 82–125 (1962).

G. Fine and E. Stolper, "The speciation of carbon dioxide in sodium aluminosilicate glasses," Contrib. Mineral. Petrol. **91**, 105–112 (1985).

R. A. Fogel "Nitrogen solubility in aubrite and E-chondrite melts," Abstr. 25th LPSC, 383–384 (1994).

D. J. Frost, U. Mann, Y. Asahara, and D. C. Rubie, "The redox state of the mantle during and just after core formation," Phil. Trans. Royal Soc. A **366**, 4315–4337 (2008).

E. M. Galimov, "Phenomenon of life: equilibrium and nonlinearity," Origins of Life and Evolution of the Biosphere **34** (6), 599–613 (2004).

E. M. Galimov, "Redox evolution of the Earth caused by a multistage formation of its core," Earth Planet. Sci. Lett. **233**, 263–276 (2005).

C. K. Gessman, B. J. Wood, D. C. Rubie, and M. R. Kilburn, "Solubility of silicon in liquid metal at high pressure: implications for the composition of the Earth's core," Earth Planet. Sci. Lett. **184**, 367–376 (2001).

D. E. Harlov, M. Andrut, and S. Melzer, "Characterization of NH_4-phlogopite $(NH_4)(Mg_3)[AlSi_3O_{10}](OH)_2$ and ND_4-phlogopite $(ND_4)(Mg_3)[AlSi_3O_{10}](OD)_2$ using IR spectroscopy and Rietveld refinement of XRD spectra," Phys. Chem. Min. **28** (2), 77–78 (2001a).

D. E. Harlov, M. Andrut, and B. Pöter,"Characterization of tobelite $(NH_4)Al_2[AlSi_3O_{10}](OH)_2$ and ND_4-tobelite $(ND_4)Al_2[AlSi_3O_{10}](OD)_2$ using IR spectroscopy and Rietveld refinement of XRD spectra," Phys. Chem. Min. **28** (4), 268–276 (2001b).

M. Hasegawa and T. Yagi, "Systematic study of formation and crystal structure of 3d-transition metal nitrides synthesized in a supercritical nitrogen fluid under 10 GPa and 1800 K using diamond anvil cell and YAG laser heating," J. Alloys Compd. **403**, 131–142 (2005).

G. Herzberg, *Molecular Spectra and Molecular Structure Vol. 2: Infrared and Raman Spectra of Polyatomic Molecules* (Van Nostrand, Princeton, 1966).

M. M. Hirschmann, "Magma ocean influence on early atmosphere mass and composition," Earth Planet. Sci. Lett. **341–344**, 48–57 (2012).

M. M. Hirschmann and A. C. Withers, "Ventilation of CO_2 from a reduced mantle and consequences for the early

martian greenhouse," Earth Planet. Sci. Lett. **270**, 147–155 (2008).

M. M. Hirschmann, A. C. Withers, P. Ardia, and N. T. Foley, "Solubility of molecular hydrogen in silicate melts and consequences for volatile evolution of terrestrial planets," Earth Planet. Sci. Lett. **345–348**, 38–48 (2012).

J. R. Holloway, "Volatile interactions in magmas," in *Advances in Physical Geochemistry*, Ed. by R.S. Newton, A. Navrotsky, and B.J. Wood (Springer, New York, 1981), pp. 273–293.

J. R. Holloway and S. Jakobsson, "Volatile solubilities in magmas: transport of volatiles from mantles to planet surface," J. Geophys. Res. **91**, D505–D508 (1986).

R. Hultgren, P. D. Desai, D. T. Hawkins, M. Gleiser, and K. K. Kelley,"Selected values of the thermodynamic properties of binary alloys," (American Society for Metals, Metals Park, Ohio, 1973).

M. Javoy, "The major volatile elements of the Earth: their origin, behavior, and fate," Geophys. Res. Lett. **24**, 177–180 (1997).

M. Javoy, E. Kaminski, F. Guyot, D. Andrault, C. Sanloup, M. Moreiraa, S. Labrosse, A. Jambon, P. Agrinier, A. Davaille, and C. Jaupart, "The chemical composition of the Earth: enstatite chondrite models," Earth Planet. Sci. Lett. **293**, 259–268 (2010).

A. A. Kadik and O. A. Lukanin, "Outgassing of the outer shells of the planets under magma-ocean conditions," Geochem. Int. **23** (6), 131–138 (1986).

A. A. Kadik, F. Pineau, Y. A. Litvin, N. Jendrzejewski, I. Martinez, and M. Javoy, "Formation of carbon and hydrogen species in magmas at low oxygen fugacity during fluid-absent melting of carbon-bearing mantle," J. Petrol. **45** (7), 1297–1310 (2004).

A. A. Kadik, N. A. Kurovskaya, Yu. A. Ignat'ev, N. N. Kononkova, V. V. Koltashev, and V. G. Plotnichenko,"Influence of oxygen fugacity on the solubility of carbon and hydrogen in $FeO–Na_2O–Al_2O_3–SiO_2$ melts in equilibrium with liquid iron at 1.5 GPa and 1400°C," Geochem. Int. **48** (10), 953–960 (2010).

A. A. Kadik, N. A. Kurovskaya, Yu. A. Ignat'ev, N. N. Kononkova, V. V. Koltashev, and V. G. Plotnichenko,"Influence of oxygen fugacity on the solubility of nitrogen, carbon, and hydrogen in $FeO–Na_2O–SiO_2–Al_2O_3$ melts in equilibrium with metallic iron at 1.5 GPa and 1400°C," Geochem. Int. **49** (5), 429–438 (2011).

A. A. Kadik, Yu. A. Litvin, V. V. Koltashev, E. B. Kryukova, V. G. Plotnichenko, T. I. Tsekhonya, and N. N. Kononkova, "Solution behavior of reduced N–H–O volatiles in $FeO–Na_2O–SiO_2–Al_2O_3$ melt equilibrated with molten Fe alloy at high pressure and temperature," Phys. Earth Planet. Int. **214**, 14–24 (2013).

A. A. Kadik, V. V. Koltashev, E. B. Kryukova, V. G. Plotnichenko, T. I. Tsekhonya, and N. N. Kononkova, "Solution behavior of C–O–H volatiles in $FeO–Na_2O–SiO_2–Al_2O_3$ melts in equilibrium with liquid iron alloy and graphite at 4 GPa and 1550°C," Geochem. Int. 52(9), 707–725 (2014).

J. F. Kerridge, "Carbon, hydrogen and nitrogen in carbonaceous chondrites: Abundances and isotopic compositions in bulk samples," Geochim. Cosmochim. Acta **49**, 1707–1714 (1985).

S.C. Kohn, R. A. Brooker, and R. Dupree, "^{13}C MAS NMR: a method for studying CO_2 speciation in glasses," Geochim. Cosmochim. Acta **55**, 3879–3884 (1991).

T. Kowal, "Anharmonic, vibrational spectra of hydroxylamine and its ^{15}N, ^{18}O, and deuterium substituted analogs," Spectrochim. Acta **58**, 1055–1067 (2002).

J. Li and C. B. Agee, "Geochemistry of mantle–core differentiation at high pressure," Nature **381**, 686–689 (1996).

Y. Li and H. Keppler, "Nitrogen speciation in mantle and crustal fluids," Geochim. Cosmoch. Acta **129**, 13–32 (2014)

Y. Li, M. Wiedenbeck, S. Shcheka, and H. Keppler, "Nitrogen solubility in upper mantle minerals," Earth Planet. Sci. Lett. **377–378**, 331–378 (2013).

Y. Li, R. Huang, M. Wiedenbeck, and H. Keppler, "Nitrogen distribution between aqueous fluids and silicate melts," Earth Planet. Sci. Lett. **411**, 218–228 (2015).

G. Libourel, B. Marty, and F. Humbert, "Nitrogen solubility in basaltic melt. Part I. Effect of oxygen fugacity," Geochim. Cosmochim. Acta **67**, 4123–4135 (2003).

Yu. A. Litvin, "Distribution of pressure up to 40 kbar and temperature up to 1500°C in the solid-state cell of large useful volume," Pribory Tekhnika Experimenta (Instruments and Technics for Experiment), No. 5, 207–209 (1979).

Yu. A. Litvin, *Physico-Chemical Study of Melting Relations of the Deep-Seated Earth's Substance* (Nauka, Moscow, 1991) [in Russian].

A. Lofthus and P. H. Krupenie, "The spectrum of molecular nitrogen," J. Phys. Chem. Ref. Data **6**, 113–307 (1977).

R. W. Luth, B. O. Mysen, and D. Virgo, "Raman spectroscopic study of the behavior of H_2 in the system $Na_2O–Al_2O_3–SiO_2–H_2$," Am. Mineral. **72**, 481–486 (1987).

Z. Ma, "Thermodynamic description for concentrated metallic solutions using interaction parameters," Metal. Mater. Trans. B **32B**, 87–103 (2001).

C. W. Mandeville, J. D. Webster, M. J. Rutherford, B. E. Taylor, A. Timbal, and K. Faure, "Determination of extinction coefficients for infrared absorption bands of H_2O in andesitic glasses," Am. Mineral. **87**, 813–821 (2002).

B. Marty, "Nitrogen content of the mantle inferred from N_2–Ar correlation in oceanic basalts," Nature **377**, 326–329 (1995).

B. Marty, "The origins and concentrations of water, carbon, nitrogen and noble gases on Earth," Earth Planet. Sci. Lett. **313–314**, 56–66 (2012).

B. Marty and N. Dauphas, "The nitrogen record of crust–mantle interaction and mantle convection from Archean to present," Earth Planet. Sci. Lett. **206**, 397–410 (2003).

M. Mercier, A. Di Muro, N. Metrich, D. Giordano, O. Belhadj, Ch. W. Mandeville, "Spectroscopic analysis (FTIR, Raman) of water in mafic and intermediate glasses and glass inclusions," Geochim. Cosmochim. Acta **74**, 5641–5656 (2010).

A. Miyazaki, H. Hiyagon, N. Sugiura, K. Hirose, and E. Takahashi, "Solubilities of nitrogen and noble gases in silicate melts under various oxygen fugacities: impli-

cations for the origin and degassing history of nitrogen and noble gases in the Earth," Geochim. Cosmochim. Acta **68**, 387–401 (2004).

Y. Morizet, M. Paris, F. Gaillard, and B. Scaillet, "C–O–H fluid solubility in haplobasalt under reducing conditions: an experimental study," Chem. Geol. **279**, 1–16 (2010).

B. O. Mysen, "Silicate–COH melt and fluid structure, their physicochemical properties, and partitioning of nominally refractory oxides between melts and fluids," Lithos **148**, 228–246 (2012).

B. O. Mysen, "Structure–property relationships of COHN-saturated silicate melt coexisting with COHN fluid: a review of in-situ, high-temperature, high-pressure experiments," Chem. Geol. **346**, 113–124 (2013).

B. O. Mysen and M. L. Fogel, "Nitrogen and hydrogen isotope compositions and solubility in silicate melts in equilibrium with reduced (N + H)-bearing fluids at high pressure and temperature: effects of melt structure," Am. Mineral. **95**, 987–999 (2010).

B. O. Mysen and P. Richet, *Silicate Glasses and Melts: Properties and Structure* (Elsevier, Amsterdam–Boston–London–New York, 2005), Developments in Geochemistry **10** (2005).

B. O. Mysen and D. Virgo, "Volatiles in silicate melts at high pressure and temperature: 2. Water in melts along the join $NaAlO_2$–SiO_2 and a comparison of solubility mechanisms of water and fluorine," Chem. Geol. **57**, 333–358 (1986).

B. O. Mysen and S. Yamashita, "Speciation of reduced C–O–H volatiles in coexisting fluids and silicate melts determined in-situ to 1.4 GPa and 800°C," Geochim. Cosmochim. Acta **74**, 4577–4588 (2010).

B. O. Mysen, S. Yamashita, and N. Cherikova, "Solubility and solution mechanisms of NOH volatiles in silicate melts at high pressure and temperature—amine groups and hydrogen fugacity," Am. Mineral. **93**, 1760–1770 (2008).

B. O. Mysen, M. L. Fogel, G. D. Cody, and P. L. Morrill, "Solution behavior of reduced C–O–H volatiles in silicate melts at high pressure and temperature," Geochim. Cosmochim. Acta **73**, 1696–1710 (2009).

B. O. Mysen, K. Kumamoto, G. D. Cody, and M. L. Fogel, "Solubility and solution mechanisms of C–O–H volatiles in silicate melt with variable redox conditions and melt composition at upper mantle temperatures and pressures," Geochim.Cosmochim. Acta **75**, 6183–6199 (2011).

B. O. Mysen, T. Tomita, Eiji Ohtani, and A. Susuki, "Speciation of and D/H partitioning between fluids and melts in silicate–D–O–H–C–N systems determined in-situ at upper mantle temperatures, pressures, and redox conditions," Am. Mineral. **99**, 578–588 (2014).

K. Nakamoto, *Infrared and Raman Spectra of Inorganic and Coordination Compounds*, 3rd ed. (John Wiley and Sons, New York, 1978).

M. Nowak and H. Behrens, "The speciation of water in haplogranitic glasses and melts by in-situ, near-infrared spectroscopy," Geochim. Cosmochim. Acta **59**, 3445–3450 (1995).

J. D. Pasteris, J. C. Seitz, B. Wopenka, and I.-M. Chou, "Recent advances in the analysis and interpretation of C–O–H–N fluids by application of laser Raman microspectroscopy," in *Microbeam Analysis*, Ed. by R. H. Geiss (San Francisco Press, San Francisco, 1990), pp. 228–234.

V. G. Plotnichenko, S. A. Vasiliev, A. O. Rybaltovskii, V. V. Koltashev, V. O. Sokolov, S. N. Klyamkin, O. I. Medvedkov, A. A. Rybaltovskii, A. R. Malosiev, and E. M. Dianov, "Hydrogen diffusion and ortho-para conversion in absorption and Raman spectra of germanosilicate optical fibers hydrogen-loaded at 150–170 MPa," J. Non-Crystal. Sol. **351** (49–51), 3677–3684 (2005).

A. Ricolleau, Y. Fei, A. Corgne, S. Julien, and B. J. James "Oxygen and silicon contents of Earth's core from high pressure metal–silicate partitioning experiments," Earth Planet. Sci. Lett. **310**, 409–421 (2011).

K. Righter and M. J. Drake, "Metal/silicate equilibrium in the early Earth—New constraints from the volatile moderately siderophile elements Ga, Cu, P, and Sn," Geochim. Cosmochim. Acta **64**, 3581–3597 (2000).

M. Roskosz, B. O. Mysen, and G. D. Cody, "Dual speciation of nitrogen in silicate melts at high pressure and temperature: an experimental study," Geochim. Cosmochim. Acta **70**, 2902–2918 (2006).

M. Roskosz, M. A. Bouhifd, A. P. Jephcoat, B. Marty, and B. O. Mysen, "Nitrogen solubility in molten metal and silicate at high pressure and temperature," Geochim. Cosmochim. Acta **121**, 15–28 (2013).

D. C. Rubie, D. J. Frost, U. Mann, Y. Asahara, F. Nimmo, K. Tsuno, P. Kegler, A. Holzheid, and H. Palme, "Heterogeneous accretion, composition and core–mantle differentiation of the Earth," Earht Planet. Sci. Lett. **301**, 31–42 (2011).

B. C. Schmidt, F. M. Holtz, and J.-M. Beny, "Incorporation of H_2 in vitreous silica, qualitative and quantitative determination from Raman and infrared spectroscopy," J. Non-Crystal. Sol. **240**, 91–103 (1998).

B. Schrader, *Raman/Infrared Atlas of Organic Compounds*, 2 ed. (VCH-Verl.-Ges., Weinheim, 1989).

J. C. Seitz, J. D. Pasteris, and B. Wopenka, "Characterization of CO_2–CH_4–H_2O fluid inclusions by microthermometry and laser Raman microprobe spectroscopy: inferences for clatrate and fluid equilibria," Geochim. Cosmochim. Acta **51**, 1651–1664 (1987).

G. H. Shaw, "Earth's atmosphere—Hadean to Early Proterozoic," Chem. Earth. Geochem. **68**, 235–264 (2008).

J. E. Shelby, "Protonic species in vitreous silica," J. Non-Crystal. Sol. **179**, 138–147 (1994).

V. K. Smirnov, A. V. Sobolev, V. G. Batanova, M. V. Portnyagin, S. G. Simakin, and E. V. Potapov, "Quantitative SIMS analysis of melt inclusions and host minerals for trace elements and H_2O," EOS Trans—Spring Meet. Suppl. AGU **76** (17), 270 (1995).

A. V. Sobolev and M. Chaussidon, "H_2O concentrations in primary melts from supra-subduction zones and mid-oceanic ridges: Implications for H_2O storage and recycling in the mantle," Earth Planet. Sci. Lett **137**, 45–55 (1996).

G. Socrates, *Infrared and Raman Characteristic Group Frequencies—Tables and Charts* (Wiley, New York, 2001).

B. D. Stanley, M. M. Hirschmann, and A. C. Withers, "Solubility of C–O–H volatiles in graphite-saturated martian basalts," Geochim. Cosmochim. Acta **129**, 54–76 (2014).

E. Stolper, "The speciation of water in silicate melts," Geochim. Cosmochim. Acta **46**, 2609–2620 (1982).

S. Takahashi, E. Ohtani, H. Terasaki, Y. Ito, Y. Shibazaki, M. Ishii, K. Funakoshi, and Y. Higo, "Phase relations in the carbon-saturated C–Mg–Fe–Si–O system and C and Si solubility in liquid Fe at high pressure and temperature: implications for planetary interiors," Phys. Chem. Minerals **40**, 647–657 (2013).

W. R. Taylor and S. F. Foley, "Improved oxygen—buffering techniques for C–O–H fluid-saturated experiments at high pressure," Geophys. Res. Lett. **94** (B4), 4146–4158 (1989).

J. H. S. Wang, D. E. Oates, A. BenReuven, and S. G. Kukolich, "Measurements of relaxation cross sections for NH3 and OCS with a molecular beam maser spectrometer," J. Chem. Phys. **59**, 5268 (1973).

A. Watenphul, B. Wunder, and W. Heinrich, "High-pressure ammonium-bearing silicates: Implications for nitrogen and hydrogen storage in the Earth's mantle," Am. Mineral. **94**, 283–292 (2009).

A. Watenphul, B. Wunder, R. Wirth, and W. Heinrich, "Ammonium-bearing clinopyroxene: a potential nitrogen reservoir in the Earth's mantle," Chem. Geol. **270**, 240–248 (2010).

D. T. Wetzel, S. D. Jacobsen, M. J. Rutherford, E. H. Hauri, and A. E. Saal, "Degassing of reduced carbon from planetary basalts," Proc. Natl. Acad. Sci. (2013). http://dx.doi.org/10.1073/ pnas.1219266110

B. J. Wood, "Carbon in the core," Earth Planet. Sci. Lett. **117**, 593–607 (1993).

B. J. Wood, M. J. Walter, and J. Wade "Accretion of the Earth and segregation of its core," Nature **441**, 825–833 (2006).

G. A. Yeo and T. A. Ford, "Ab initio molecular orbital calculations of the energetic, structural, vibrational, and electronic properties of some hydrogen bonded complexes of water, ammonia and hydroxylamine," Spectrochim. Acta **50A**, 5–18 (1994).

K. J. Zahnle, "Earth's earliest atmosphere," Elements **2**, 217–222 (2006).

K. Zahnle, L. Schaefer, and B. Fegley, "Earth's earliest atmosphere," Cold Spring Harb. Perspect Biol. **2** (10), a004895 (2010). doi 10.1101/cshperspect.a004895

Translated by A. Girnis